

# Total Synthesis and Biological Evaluation of the Fab-Inhibitory Antibiotic Platencin and Analogues Thereof

Gulice Y. C. Leung,<sup>[a]</sup> Hao Li,<sup>[a]</sup> Qiao-Yan Toh,<sup>[a]</sup> Amelia M.-Y. Ng,<sup>[a]</sup> Rong Ji Sum,<sup>[a]</sup> Julia E. Bandow,<sup>[b]</sup> and David Y.-K. Chen<sup>\*[a]</sup>

**Keywords:** Total synthesis / Natural products / Antibiotics / Medicinal chemistry

In this article, application of the masked *o*-benzoquinone intramolecular Diels–Alder reaction in the total synthesis of platencin (**2**), a recently reported Fab inhibitory antibiotic, is described. Through intelligence gathering, the evolving strategies ultimately culminated in three syntheses of the tricyclic core structure **11** of platencin (**2**). The influence of the remote stereocenter(s) in the diastereoselectivity of the intramolecular Diels–Alder reaction was investigated, together

with a remarkable additive effect in drastically improving the diastereoselectivity of the intramolecular Diels–Alder reaction of the dienone **17**. The synthetic technology developed was further applied to the preparation of rationally designed analogues, based on the hypothesized FabF/FabH selectivity model. Antibacterial studies of platencin (**2**) and of the synthesized analogues **3–9** against a panel of normal and resistant strains are also reported.

## Introduction

The combat against infectious diseases continue to assume a high priority on the global health agenda.<sup>[1]</sup> In particular, escalating reports of multidrug resistance (MDR) threaten the eventually obsolescence of existing therapies.<sup>[2]</sup> This crisis, according to experts, could take us back to the so-called “dark age” of the pre-antibiotic era. Several factors may contribute to the development of MDR, but it is commonly the consequence of over-exposure to antibiotic agents and evolutionary natural selection on the bacterial life cycle. Over-prescribing of antibiotics, incorrect prescription of antibiotics for viral infections, and increasing usage of agricultural antibiotics are all sources of over-exposure. Furthermore, patients immunocompromised through prolonged chemotherapy are also more susceptible to new bacterial infections. As such, efforts in the discovery and development of antibiotics with novel mechanisms of action must continue in order to combat this unmet and recurring medical emergency.<sup>[3]</sup>

Fatty acid biosynthesis (Fab) is an essential metabolic process for all living organisms.<sup>[4]</sup> Indeed, inhibitors tar-

getting the various stages of the fatty acid biosynthetic pathway have been investigated as novel antibacterial agents.<sup>[5]</sup> Recently, the discovery of platensimycin (**1**, Figure 1) and platencin (**2**, Figure 1) by the Merck team beautifully illustrated the state-of-the-art technology in the identification of novel Fab inhibitors.<sup>[6,7]</sup> In a combination of classical high-throughput screening (HTS) of natural product extracts and the application of the RNA silencing technology (RNAi), platensimycin (**1**) and platencin (**2**) were identified as potent and selective inhibitor and dual inhibitor of the fatty-acid condensing enzymes FabF and FabF/FabH, respectively.<sup>[6a,7a]</sup> It has been suggested that the *o*-hydroxybenzoic acid moiety of platensimycin and platencin mimics and competes with the natural  $\beta$ -ketoacyl (acyl-carrier protein) substrate, thereby terminating the elongation-condensing step in the Fab pathway.<sup>[6a,7a]</sup> Furthermore, molecular docking studies have suggested the relevance of the ether oxygen (Figure 1, **1**, O<sup>16</sup>) in platensimycin and the exocyclic methylene (Figure 1, **2**, C<sup>15</sup>–C<sup>16</sup>) in platencin for the observed FabF/FabH selectivity.<sup>[7b]</sup> Because these enzymes are highly conserved among the clinically relevant pathogens, platensimycin (**1**) and platencin (**2**) display broad-spectrum antibiotic activities, including activities against the resistant strains MRSA (methicillin-resistant *S. aureus*) and VRE (vancomycin-resistant enterococci).<sup>[6a,7a]</sup> However, in vivo efficacy of platensimycin (**1**) could only be achieved by continuous parenteral infusion at high dose.<sup>[6a]</sup> The clinical utility of platensimycin (**1**) and platencin (**2**) is therefore yet to be demonstrated with greatly improved pharmacokinetic profile, and one such way of achieving this is through the preparation of rationally designed analogues.

[a] Chemical Synthesis Laboratory@Biopolis, Institute of Chemical and Engineering Sciences (ICES), Agency for Science Technology and Research (A\*STAR), 11 Biopolis Way, The Helios Block, #03-08, Singapore 138667  
E-mail: david\_chen@ices.a-star.edu.sg

[b] Lehrstuhl für Biologie der Mikroorganismen, Fakultät für Biologie und Biotechnologie, Ruhr-Universität Bochum, Universitätsstrasse 150, 44801 Bochum, Germany  
Fax: +49-234-3214378  
E-mail: julia.bandow@rub.de

Supporting information for this article is available on the WWW under <http://dx.doi.org/10.1002/ejoc.201001281>.

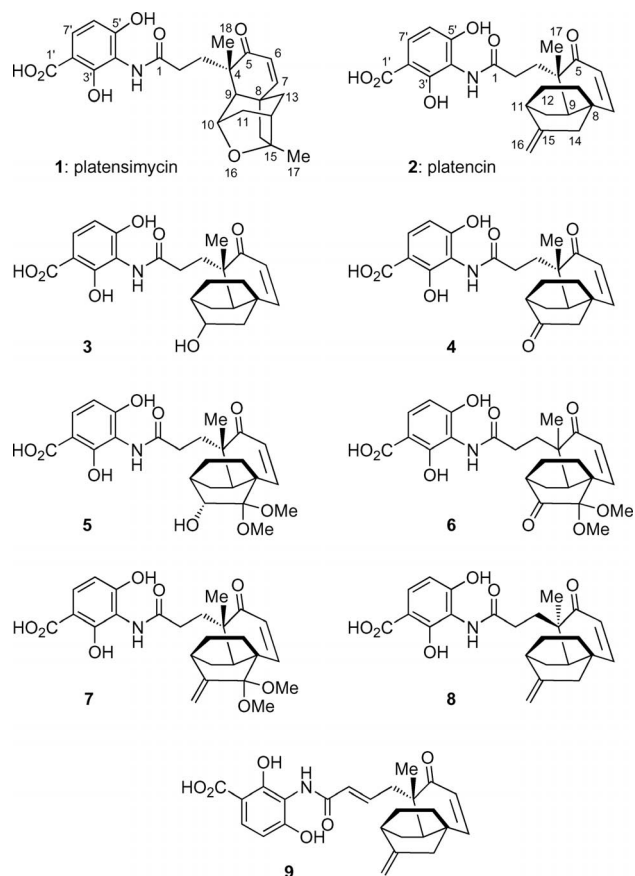


Figure 1. Structures of platensimycin (**1**), platencin (**2**), and the platencin analogues **3–9**.

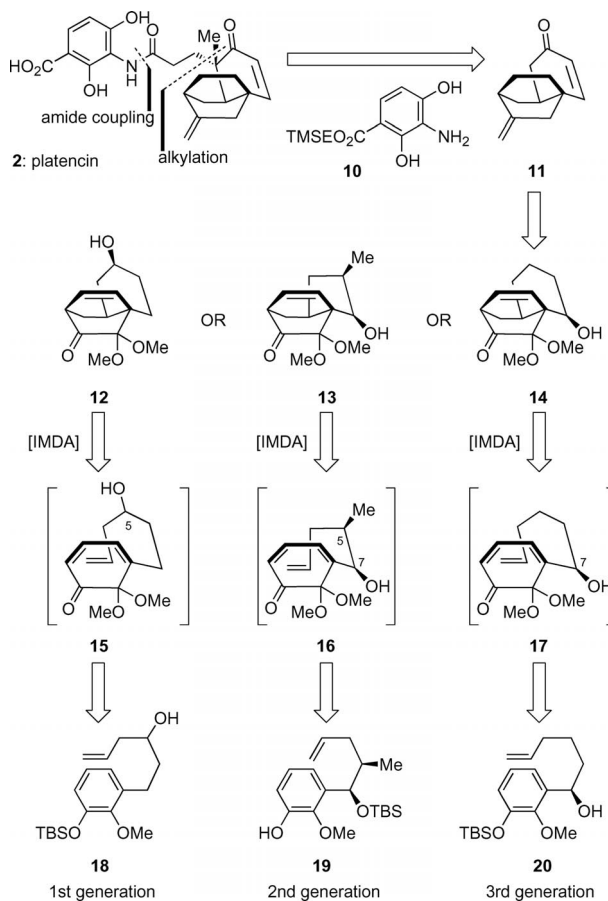
The promising therapeutic potentials and intriguing molecular architectures of platensimycin (**1**) and platencin (**2**) have attracted significant interest from both the biology and the chemistry communities, with a number of elegant syntheses<sup>[8,9]</sup> and rationally designed analogues<sup>[10]</sup> reported. Here we report the evolution of our synthetic strategy that ultimately culminated in three syntheses of platencin (**2**). In conjunction with our interest in the chemical/biology investigations of platencin (**2**), rationally designed analogues based on the hypothesized FabH/FabF selectivity model were synthesized, and their antibiotic activities against selected bacterial strains are reported.

## Results and Discussion

### Retrosynthetic Analysis

While the chemical structure of platencin (**2**) has inspired a plethora of innovative and contrasting approaches from the synthetic community,<sup>[9]</sup> detachment of the aromatic domain (**10**) at the amide bond linkage, as shown in Scheme 1, has been widely accepted as the opening retrosynthetic maneuver. Further retrosynthetic disassembly of platencin (**2**) was achieved through the recognition of the inherent facial bias exhibited by its rigid cage structure, in which the sequential introduction of the two side chains (C<sup>17</sup> methyl

and C<sup>1</sup>–C<sup>3</sup> propanoic acid) would be expected to take place stereoselectively, leading to the tricyclic enone **11** as a suitable precursor. Indeed, this stereoselective double alkylation was first demonstrated by Nicolaou's group in their total synthesis of (±)-platencin (**2**).<sup>[9a]</sup>



Scheme 1. Retrosynthetic analysis of platencin (**2**) leading to the alkenyl diphenols **18**, **19** and **20**. TMSE = trimethylsilylethyl, TBS = *tert*-butyldimethylsilyl, IMDA = intramolecular Diels–Alder.

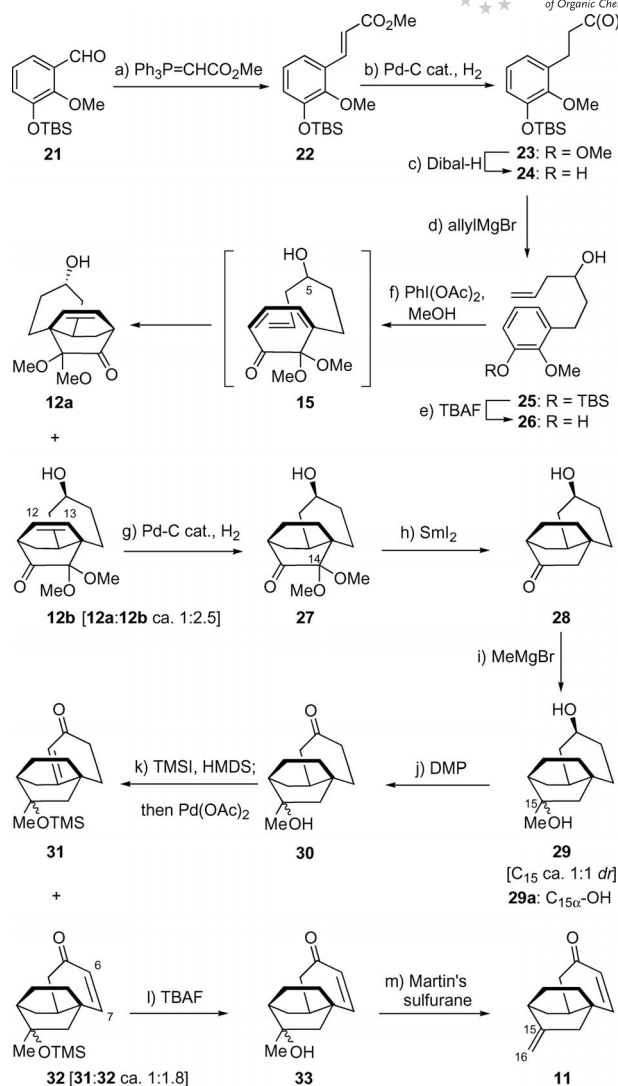
With tricyclic enone **11** in mind, an intramolecular Diels–Alder reaction<sup>[11]</sup> was conceived for its construction. Inspired by the work of Liao and co-workers in the intramolecular cycloaddition reactions of masked *o*-benzoquinones,<sup>[12]</sup> 6,6-dimethoxycyclohexa-2,4-dienone bearing pendent terminal alkenes, as represented by the structures **15**, **16** and **17**, originating from oxidative dearomatization of desilylated versions of the aromatic phenols **18**, **19** and **20**, respectively, were proposed as suitable intramolecular Diels–Alder precursors. In order to access the targeted tricyclic **11** stereoselectively through the proposed intramolecular Diels–Alder reaction, we envisaged the application of remote stereocontrol, in which the stereochemical information residing in the acyclic alkenyl side chain (C<sub>5</sub> in **15**, C<sub>5</sub>, C<sub>7</sub> in **16** and C<sub>7</sub> in **17**) would be expected to translate to the cycloaddition adduct through a well-ordered transition state (**15**, **16** or **17**). Through intelligence gathering, this generalized synthetic plan ultimately culminated in three

syntheses of the tricyclic enone **11**, as discussed in the following sections and illustrated in Schemes 2, 3, 4, 5 and 6, below.

### First-Generation Synthesis of the Tricyclic Enone **11**

We began our investigation into the intramolecular Diels–Alder reaction of substrate **15** and the stereochemical outcome of this process, influenced by its C<sub>5</sub> hydroxy substituent (platencin numbering), as shown in Scheme 2. The preparation of the intramolecular Diels–Alder precursor **15** commenced with a two-carbon homologation of the aldehyde **21**<sup>[13]</sup> [(MeO)<sub>2</sub>P(O)CH<sub>2</sub>CO<sub>2</sub>Me], followed by catalytic hydrogenation (H<sub>2</sub>, cat. Pd-C) and Dibal-H reduction of the resulting methyl ester **23** to afford the aldehyde **24** in 60% overall yield for the three steps. Treatment of the aldehyde **24** with allylmagnesium bromide with subsequent desilylation (TBAF) provided the phenol **26** (70% overall yield from **24**), ready for oxidative dearomatization and the proposed intramolecular Diels–Alder reaction. In this instance, oxidative dearomatization of the phenol **26** through the action of PhI(OAc)<sub>2</sub> in MeOH, by the protocol developed by Liao and co-workers,<sup>[12]</sup> smoothly delivered the dimethoxy cyclohexadienone **15** as a single detectable product. This species proved stable to aqueous workup and was subjected to thermal conditions after solvent exchange (MeOH to toluene), to furnish the intramolecular Diels–Alder products **12a** and **12b** as a separable mixture of two diastereoisomers (*dr* ≈ 1:2.5 by <sup>1</sup>H NMR analysis) in 64% combined yield. The diastereoisomeric relationship between **12a** and **12b** was corroborated through oxidation of its secondary hydroxy group, either as a diastereoisomeric mixture or isomerically pure material, to deliver a single diketone (**12c**, 87% yield, see the Supporting Information). Furthermore, the structure of the Diels–Alder product **12b** (and therefore of **12a**) was indirectly validated through X-ray crystallographic analysis of a later intermediate (**29a**, Figure 3). The preferential formation of the Diels–Alder product **12b** over **12a** could be interpreted on the basis of chair-like transition state models as illustrated in Figure 2, in which the transition state **I** would be energetically disfavoured due to its axially positioned C<sub>5</sub> hydroxy group exhibiting steric and electrostatic repulsion with the dimethyl acetal moiety. The conformation of the newly formed six-membered ring bearing the C<sub>5</sub> hydroxy group, as depicted in the X-ray crystallographic structure of **29a** (Figure 3) derived from the major Diels–Alder product **12b**, also supports the hypothesized transition state **II**. The modest level of diastereoselectivity in favour of **12b** is probably due to the C<sub>5</sub> hydroxy directing group being positioned four carbons away from the dimethoxy acetal moiety, the steric and electrostatic repulsion therefore not being severe enough to induce a greater energetic bias between **I** and **II**.

Although the stereochemical outcome of this intramolecular Diels–Alder reaction proved inconsequential in the racemic synthesis of the enone **11**, it has an important implication in the asymmetric setting. In this context, if enantio-



Scheme 2. First-generation synthesis of the enone **11**. Reagents and conditions: a) trimethylphosphonoacetate (1.2 equiv.), LiBr (4.0 equiv.), Et<sub>3</sub>N (2.0 equiv.), THF, 23 °C, 5 h, 70%; b) Pd-C (0.25 equiv.), H<sub>2</sub>, MeOH, 23 °C, 30 min, 90%; c) Dibal-H (1.0 M in toluene, 1.0 equiv.), CH<sub>2</sub>Cl<sub>2</sub>, -78 °C, 1 h, 96%; d) allylmagnesium bromide (1.0 M in THF, 1.2 equiv.), THF, -78 °C, 2 h, 81%; e) TBAF (1.0 M in THF, 1.1 equiv.), THF, 23 °C, 2 h, 87%; f) PhI(OAc)<sub>2</sub> (1.1 equiv.), KHCO<sub>3</sub> (2.0 equiv.), MeOH, 0 → 23 °C, 30 min; then toluene, reflux, 4 h, 64% (ca. 2.5:1 mixture of diastereoisomers by <sup>1</sup>H NMR); g) Pd-C (0.25 equiv.), H<sub>2</sub>, MeOH, 23 °C, 30 min, 89%; h) SmI<sub>2</sub> (0.1 M in THF, 4.0 equiv.), THF/MeOH (20:1), 23 °C, 30 min, 95%; i) MeMgBr (1.0 M in THF, 2.2 equiv.), THF, -78 °C, 2 h, 86% (ca. 1:1 mixture of diastereoisomers by <sup>1</sup>H NMR); j) DMP (1.0 equiv.), NaHCO<sub>3</sub> (1.2 equiv.), CH<sub>2</sub>Cl<sub>2</sub>, 23 °C, 2 h, 85%; k) TMSI (2.0 equiv.), HMDS (3.0 equiv.), CH<sub>2</sub>Cl<sub>2</sub>, 0 → 23 °C, 6 h; then Pd(OAc)<sub>2</sub> (1.0 equiv.), CH<sub>3</sub>CN, 23 °C, 5 h, **32**: 64%, **31**: 35%; l) TBAF (1.0 M in THF, 1.1 equiv.), THF, 23 °C, 2 h, 98%; m) Martin's sulfurane (2.0 equiv.), CH<sub>2</sub>Cl<sub>2</sub>, 23 °C, 2 h, 90%. Dibal-H = diisobutylaluminium hydride, TBAF = tetra-*n*-butylammonium fluoride, DMP = Dess–Martin periodinane, TMS = trimethylsilyl, HMDS = hexamethyldisilazane.

merically enriched alcohol **15** were employed, the poor diastereoselection associated with the intramolecular Diels–Alder process would lead to significant reduction in the optical purity of the ensuing intermediates upon removal of

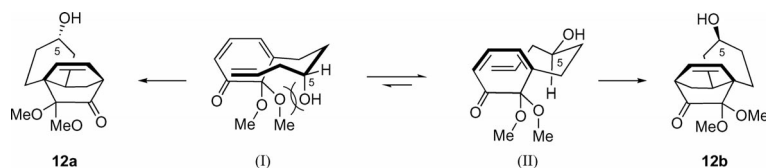


Figure 2. Proposed transition state structures **I** and **II** leading to the Diels–Alder products **12a** and **12b**, respectively.

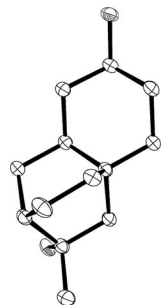


Figure 3. X-ray-derived ORTEP diagram of the diol **29a** with thermal ellipsoids shown at the 50% probability level.<sup>[14]</sup>

the C<sub>5</sub> hydroxy chiral centre. At this point, we arbitrarily chose the tricyclic compound **12b**, and its advancement to the targeted enone **11** was pursued in earnest. Hydrogenation of the alkene **12b** (H<sub>2</sub>, Pd-C) and removal of the dimethyl acetal (SmI<sub>2</sub>)<sup>[15]</sup> in compound **27** afforded the hydroxy ketone **28** in 85% yield over the two steps. Grignard addition of a methyl group at ketone **28** resulted in the diol **29**, inconsequentially as an epimeric mixture at the C<sup>15</sup> carbinol centre [86% yield, ca. 1:1 by <sup>1</sup>H NMR spectroscopy]. X-ray analysis of the isomer **29a** [m.p. 164–167 °C (EtOAc)] confirmed its structure (Figure 3).<sup>[14]</sup> Compound **29** was subjected to DMP conditions to give the keto carbinol **30** in 85% yield.

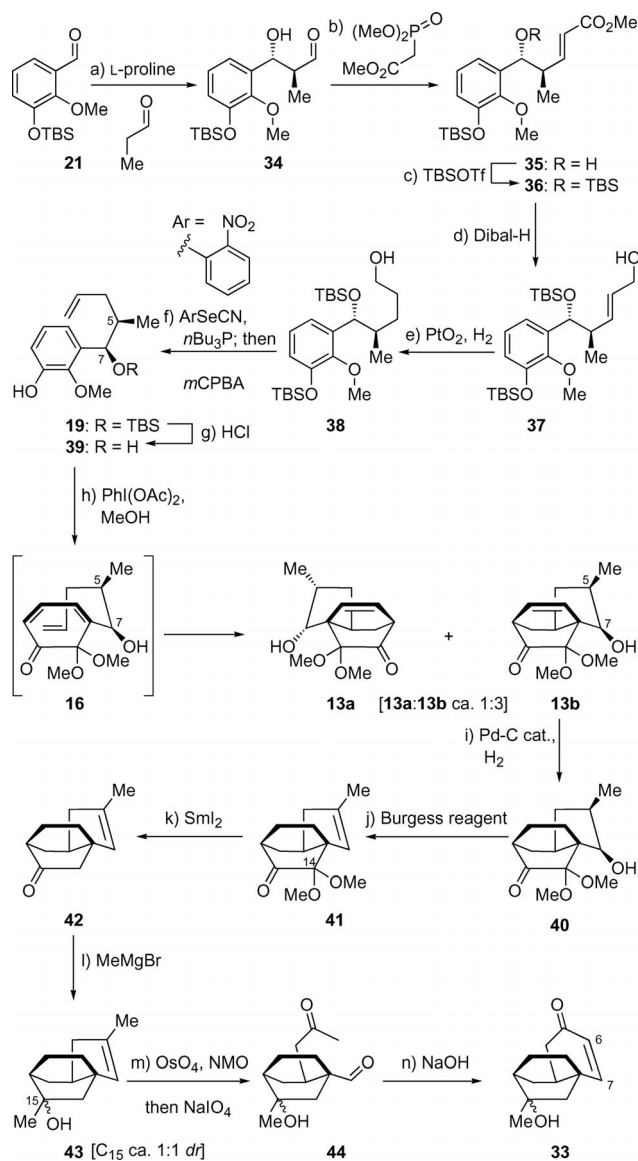
The final steps leading to the targeted tricycle **11** required the introduction of the enone moiety (C<sup>6</sup>–C<sup>7</sup>), and dehydration of the tertiary alcohol (C<sup>15</sup>) to generate the exocyclic olefin (C<sup>15</sup>–C<sup>16</sup>). The former of these two transformations was accomplished under Saegusa's conditions,<sup>[16]</sup> with subjection of a nearly 1:1.8 regioisomeric mixture of TMS silyl enol ethers derived from ketone **30** (TMSI, HMDS) to Pd(OAc)<sub>2</sub> to give a separable mixture of the two regioisomeric enones **31** and **32** in 99% combined yield (**31/32** ca. 1:1.8). Removal of the TMS ether from the major enone (**32**, TBAF, 98% yield), followed by Martin's sulfurane-mediated dehydration<sup>[17]</sup> (90% yield) completed the synthesis of the racemic tricycle **11**, the spectroscopic data (<sup>1</sup>H and <sup>13</sup>C NMR) of which identically matched those reported in the literature.<sup>[9]</sup>

### Second-Generation Synthesis of the Tricyclic Enone **11**

Although our first-generation strategy served to deliver the targeted tricyclic enone **11**, there were two major drawbacks. Firstly, as alluded to earlier, the poor diastereoselection in the intramolecular Diels–Alder reaction with the substrate **15** implied that this first-generation strategy

would not be readily amenable in an asymmetric setting. Secondly, the late-stage introduction of the enone functionality by the Saegusa protocol<sup>[16]</sup> (**30** to **31** and **32**) also suffered from poor regioselectivity in the initial TMS enol ether formation from ketone **30**. With these shortcomings in mind, a second-generation strategy was conceived and successfully executed as shown in Scheme 3. Firstly, to improve the stereoselectivity of the intramolecular Diels–Alder reaction, we hypothesized that relocation of the stereocentre to closer proximity in the intramolecular Diels–Alder transition state should provide greater energetic difference between the competing diastereoisomeric reaction pathways. Furthermore, the presence of methyl (C<sup>5</sup>) and hydroxy (C<sup>7</sup>) substituents on the alkenyl side chain should serve as handles for the late-stage, regioselective introduction of the C<sup>6</sup>–C<sup>7</sup> enone moiety.

The synthesis of the intramolecular Diels–Alder precursor **16**, bearing two neighbouring stereocentres, thus began with an L-proline-mediated aldol<sup>[18]</sup> reaction between the aromatic aldehyde **21** and propionaldehyde to give the β-hydroxy aldehyde **34** as a single diastereoisomer in 83% yield and >90% *ee* (determined by <sup>1</sup>H NMR analysis of a Mosher ester derivative of **34**; see the Supporting Information). Two-carbon homologation of the aldehyde **34** [(MeO)<sub>2</sub>P(O)CH<sub>2</sub>CO<sub>2</sub>Me, **35**], followed by silylation (TBSOTf), afforded the enoate **36** in 84% yield over the two steps. Dibal-H reduction of the enoate **36** afforded the allylic alcohol **37** (86% yield), which was subjected to catalytic hydrogenation in the presence of PtO<sub>2</sub> (99% yield) to give the primary alcohol **38**. Dehydration of **38** through its selenide derivative<sup>[19]</sup> (*o*-NO<sub>2</sub>C<sub>6</sub>H<sub>4</sub>SeCN, *n*Bu<sub>3</sub>P; then *m*CPBA, 97% yield) took place with concomitant removal of the phenolic TBS ether, and subsequent desilylation of the resulting TBS ether **19** furnished the hydroxy phenol **39** ready for the intramolecular Diels–Alder reaction. Under the previously established conditions for oxidative dearomatization [PhI(OAc)<sub>2</sub>, MeOH], the phenol **39** was smoothly converted into the dienone **16** and subsequently subjected under thermal conditions (toluene, reflux) to afford a separable mixture of the intramolecular Diels–Alder products **13a** and **13b** in 69% yield over the two steps (**13a/13b** ≈ 1:3). The diastereoisomeric relationship between **13a** and **13b** was corroborated by hydrogenation, followed by dehydrative elimination of the C<sub>7</sub> secondary hydroxy group, to deliver the enantiomeric keto olefins **41** and *ent*-**41** (see the Supporting Information). Furthermore, the structure of the Diels–Alder product **13b** (and therefore that of **13a**) was indirectly validated through X-ray crystallographic analysis of a later intermediate (**40**, see Figure 5). Analogously with the transition state models proposed for the formation of



Scheme 3. Second-generation synthesis of the enone **33**. Reagents and conditions: a) L-proline (0.1 equiv.), propionaldehyde (5.0 equiv.), DMF, 4 °C, 48 h, 83%; b) trimethylphosphonoacetate (1.2 equiv.), LiBr (3.8 equiv.), Et<sub>3</sub>N (2.0 equiv.), THF, 23 °C, 1 h, 99%; c) 2,6-lutidine (2.0 equiv.), TBSOTf (1.5 equiv.), CH<sub>2</sub>Cl<sub>2</sub>, -78 to 23 °C, 4 h, 85%; d) Dibal-H (1.0 M in toluene, 3.0 equiv.), CH<sub>2</sub>Cl<sub>2</sub>, -78 °C, 2.5 h, 86%; e) PtO<sub>2</sub> (0.2 equiv.), H<sub>2</sub> (1 atm), EtOAc, 23 °C, 20 h, 99%; f) *o*-NO<sub>2</sub>C<sub>6</sub>H<sub>4</sub>SeCN (1.4 equiv.), *n*Bu<sub>3</sub>P (2.0 equiv.), THF, 23 °C, 30 min; then *m*CPBA (2.0 equiv.), CH<sub>2</sub>Cl<sub>2</sub>, 0 °C, 1 h; then DBU (2.0 equiv.), toluene, 80 °C, 19 h, 97% for the three steps; g) HCl (6.0 M aq., 2.0 equiv.), MeOH, 23 °C, 1.5 h, 80%; h) PhI(OAc)<sub>2</sub> (1.0 equiv.), KHCO<sub>3</sub> (2.0 equiv.), MeOH, 23 °C, 1 h; then toluene, reflux, 6 h, 69% (ca. 3:1 mixture of diastereoisomers by <sup>1</sup>H NMR); i) Pd-C (0.25 equiv.), H<sub>2</sub> (1 atm), MeOH, 23 °C, 1 h, 91%; j) Burgess reagent (2.0 equiv.), toluene, reflux, 19 h, 67%; k) Sml<sub>2</sub> (0.1 M in THF, 8.0 equiv.), THF/MeOH (20:1), 23 °C, 30 min, 89%; l) MeMgBr (1.0 M in THF, 3.0 equiv.), THF, 0 °C, 17 h, 73% (ca. 1:1 mixture of diastereoisomers by <sup>1</sup>H NMR); m) OsO<sub>4</sub> (2.5 wt.-% in *t*BuOH, 0.1 equiv.), NMO (2.5 equiv.), *t*BuOH/acetone/H<sub>2</sub>O (1:1:1), 23 °C, 14 h; then NaIO<sub>4</sub> (1.5 equiv.), 23 °C, 6 h; n) NaOH (6.0 equiv.), EtOH, 23 °C, 2 h, 80% over the two steps. NMO = *N*-methylmorpholine *N*-oxide.

**12a** and **12b** [**I** and **II**, respectively], the sterically and electronically preferred transition state **IV** (conformation supported by X-ray structure of **40**; Figure 5, below) over **III** could also be conceived for the predominant formation of the Diels–Alder product **13b** (Figure 4). In contrast with the transition states **I** and **II**, in this instance, although the steric and electrostatic pressure is more severe in **III** because the C<sup>7</sup> hydroxy group is brought into closer proximity to the dimethyl acetal moiety, the steric repulsion between the C<sup>5</sup> methyl group and C<sup>7</sup> hydroxy group experienced in both **III** and **IV** might, however, have contributed to the modest level of diastereoselectivity observed for the Diels–Alder reaction of **16**. Although the modest diastereoselectivity in this second-generation intramolecular Diels–Alder reaction had once again proved disappointing, we opted to continue the elaboration of the intramolecular Diels–Alder product **13b** (arbitrarily chosen) as outlined in Scheme 3. Catalytic hydrogenation of the alkenyl ketone **13b** gave the hydroxy ketone **40** (Pd-C, H<sub>2</sub>, 91% yield), which was dehydrated in the presence of Burgess' reagent<sup>[20]</sup> to afford the alkene **41** in 67% yield. The structural identity of the hydroxy ketone **40** [m.p. 98–100 °C (hexane/EtOAc)] was confirmed by X-ray crystallographic analysis as shown in Figure 5.<sup>[21]</sup> Reductive removal of the dimethoxy substituents of **41** (SmI<sub>2</sub>)<sup>[15]</sup> furnished the ketone **42** (89% yield), which was treated with methyl Grignard reagent to afford the alkenyl carbinol **43**, inconsequentially as a mixture (C<sup>15</sup>: *dr* ≈ 1:1), in 73% yield. In contrast to the first-generation approach, the regioselective introduction of the enone moiety (C<sup>6</sup>–C<sup>7</sup>) was carried out through a dihydroxylation cleavage/aldol condensation sequence, thereby converting the alkene **43** into the enone **33**, through the intermediacy of the keto aldehyde **44**, in 80% yield over the two steps. The spectroscopic data (<sup>1</sup>H and <sup>13</sup>C NMR) for enone **33** matched those obtained in the first-generation synthesis identically, thereby constituting a formal synthesis of the platencin core structure **11** by interception of this late-stage intermediate.

### Third-Generation Synthesis of the Tricyclic Enone **11**

Our second-generation synthesis of tricyclic enone **11** had addressed the regioselective introduction of the C<sup>6</sup>–C<sup>7</sup> enone moiety, but the diastereoselectivity of the intramolecular Diels–Alder reaction unfortunately remained unsatisfactory. At this juncture we turned to the intramolecular Diels–Alder reaction of the dimethoxy-cyclohexadienone **17** (Scheme 5, a), a substrate that had previously been examined by Liao and co-workers and found to exhibit high levels of diastereoselectivity in the intramolecular Diels–Alder reaction.<sup>[12]</sup> Furthermore, with an asymmetric synthesis of the tricyclic enone **11** in mind, we envisaged that a chiral reduction of the ketone **46** (or **47**), followed by desilylation, should deliver the alcohol **51** (precursor to the dienone **17**) in its optically active form, as shown in Schemes 4 and 5 and Table 1. The ketone **46** was thus prepared from the aldehyde **21**<sup>[13]</sup> through the action of the Grignard reagent **45** and PCC oxidation of the intermediate alcohol **20**, in 78%

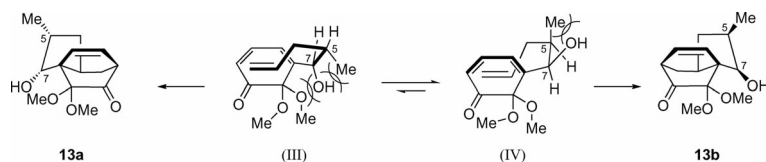


Figure 4. Proposed transition state structures **III** and **IV** leading to the Diels–Alder products **13a** and **13b**, respectively.

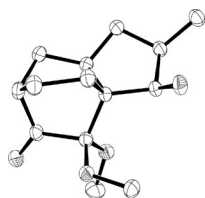
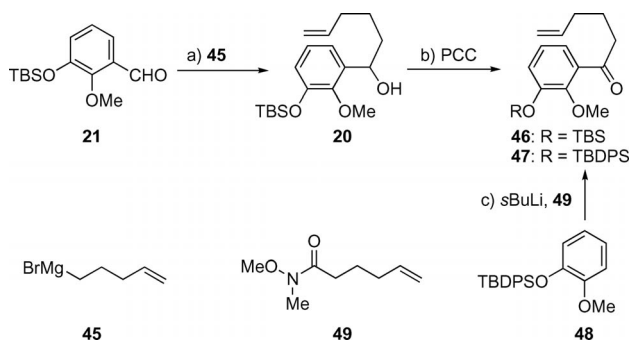


Figure 5. X-ray-derived ORTEP diagram of the hydroxy ketone **40**, with thermal ellipsoids shown at the 50% probability level.<sup>[21]</sup>

overall yield. Alternatively, the TBDPS version of ketone **46** was directly accessible from the methyl ether **48**<sup>[22]</sup> through *ortho* lithiation and treatment of the resulting aryl-lithium species with the Weinreb amide **49**<sup>[23]</sup> (**47**, 51% yield).



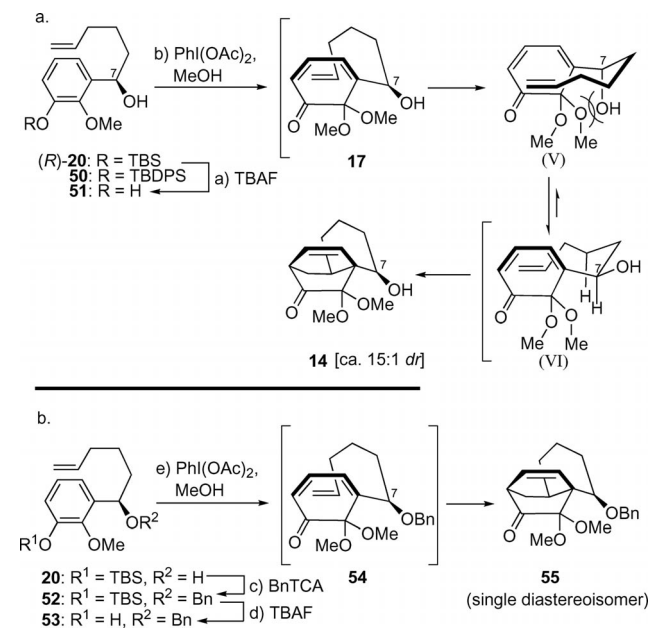
Scheme 4. Synthesis of the racemic alcohol **20** and the ketones **46** and **47**. Reagents and conditions: a) **45** (2.2 equiv.), Et<sub>2</sub>O, –10 °C, 1 h, 82%; b) PCC (1.6 equiv.), CH<sub>2</sub>Cl<sub>2</sub>, 23 °C, 16 h, 95%; c) *s*BuLi (1.4 M in cyclohexane, 1.2 equiv.), TMEDA (1.5 equiv.), THF, –78 °C, 45 min; then **49** (1.0 equiv.), –78 °C, 2 h, 51% (90% based on 57% conversion). TBDPS = *tert*-butyldiphenylsilyl, PCC = pyridinium chlorochromate, TMEDA = *N,N,N',N'*-tetramethylethylenediamine.

Table 1. Asymmetric reduction of ketones **46** and **47**.

Entry <sup>[a]</sup>	Solvent	Temperature [°C]	Time [h]	Yield [%] <sup>[e]</sup>	Recovered [%] <sup>[e]</sup>	<i>ee</i> <sup>[b]</sup> [%]
1	THF	0	2	<b>50</b> : 31	<b>47</b> : 54	67
2	THF	0	2	<b>50</b> : 55	<b>47</b> : 45	90
3	THF	0	1	<b>50</b> : 60	<b>47</b> : 40	90
4 <sup>[c]</sup>	THF	0	0.25	<b>50</b> : 41	<b>47</b> : 59	90
5	THF	23	1	<b>50</b> : 50	–	90
6	toluene	–78	8	<b>50</b> : 57	–	45
7	toluene	0	1	<b>50</b> : 58	<b>47</b> : 23	69
8	toluene	0	3	( <i>R</i> )- <b>20</b> : 58	–	89
9 <sup>[c],[d]</sup>	toluene	0	0.25	( <i>R</i> )- <b>20</b> : 99	–	90

[a] The ketone **47** was used for Entries 1–7 and the ketone **46** was used for Entries 8 and 9; BH<sub>3</sub>·SMe<sub>2</sub> was used for Entry 1 and catechol borane was used for Entries 2–9. [b] The *ee* value was determined by <sup>1</sup>H NMR analysis of the Mosher ester derivative. [c] Alternating/reverse addition protocol (see the Supporting Information), and reaction mixture was stirred for an additional 15 min upon completion of addition. [d] Reaction was performed on a 15 mmol scale. [e] Yields refer to chromatographically and spectroscopically homogeneous materials.

Asymmetric reduction of the ketone **46** (and **47**) under the CBS conditions<sup>[24]</sup> was examined next, and the results are shown in Table 1. After extensive experimentation, opti-



Scheme 5. Synthesis of the alkenyl ketones **14** and **55** through intramolecular Diels–Alder reactions. Reagents and conditions: a) TBAF (1.0 M in THF, 1.1 equiv.), THF, 0 °C, 2 h, 99% [from (*R*)-**20**], 92% [from **50**]; b) PhI(OAc)<sub>2</sub> (1.1 equiv.), KHCO<sub>3</sub> (2.0 equiv.), MeOH, 0 → 23 °C, 30 min; then toluene, reflux, 4 h, 80% (ca. 15:1 mixture of diastereoisomers by <sup>1</sup>H NMR); c) benzyl trichloroacetimidate (1.5 equiv.), TMSOTf (0.2 equiv.), CH<sub>2</sub>Cl<sub>2</sub>/hexane (1:3), 0 → 23 °C, 4 h, 76%; d) TBAF (1.0 M in THF, 3.0 equiv.), THF, 0 °C, 0.5 h, 51%; e) PhI(OAc)<sub>2</sub> (1.1 equiv.), KHCO<sub>3</sub> (2.0 equiv.), MeOH, 0 → 23 °C, 30 min; then toluene, reflux, 16 h, 73%. OTf = trifluoromethanesulfonate, BnTCA = benzyl trichloroacetimidate.

mal conversion and enantiomeric excess were achieved through a reverse-addition protocol (see the Supporting Information), and the reaction was ultimately performed on a multigram scale with excellent yield [(*R*)-**20**, 99% yield] and optical purity (90% *ee* by  $^1\text{H}$  NMR analysis of the Mosher ester derivative, Table 1, Entry 9).

With the alcohols (*R*)-**20** and **50** in hand, their conversion into the intramolecular Diels–Alder product **14** began with the removal of the silyl ether [TBAF, 99% yield from (*R*)-**20** and 92% from **50**], followed by  $\text{PhI}(\text{OAc})_2$ -mediated oxidative dearomatization, to afford the intramolecular Diels–Alder precursor **17** (Scheme 5, a). As anticipated, the intramolecular Diels–Alder reaction of **17** proceeded with high levels of conversion (80% yield) and diastereoselectivity (ca. 15:1 by  $^1\text{H}$  NMR analysis), presumably through the conformationally preferred chair-like transition state **VI** (over **V**). In contrast to the proposed transition states leading to the formation of **12a/b** and **13a/b** (**I/II** and **III/IV**), the energetic difference between **V** and **VI** is quite large, thus leading to the high observed level of diastereoselectivity. Having validated the influence of the  $\text{C}^7$  (platencin numbering) hydroxy substituent on the diastereoselectivity as reported by Liao and co-workers,<sup>[12]</sup> we hypothesized that increasing the steric bulk about this hydroxy centre should lead to a higher level of stereoinduction. This hypothesis was validated by the intramolecular Diels–Alder reaction of the benzyl ether **54**, a substrate prepared by benzylation of the alcohol **20** (benzyl trichloroacetimidate, TMSOTf cat., 76% yield) followed by silyl deprotection (TBAF, 51% yield) and oxidative dearomatization [ $\text{PhI}(\text{OAc})_2$ ], as shown in part b of Scheme 5. Indeed, heating of a toluene solution of the intramolecular Diels–Alder precursor **54** smoothly delivered the tricycle **55** as a single diastereoisomer (by  $^1\text{H}$  NMR analysis) in 73% yield.

Although the introduction of a sterically bulky substituent (e.g., Bn) at the 7-OH group served to improve the diastereoselectivity of the intramolecular Diels–Alder reaction, the installation and later removal of this protecting group was less attractive in terms of the overall synthetic efficiency. We thus became interested in the in situ generation of a species with a temporarily increased steric environment around 7-OH, which might serve a role similar to that of a covalently attached protecting group. Along this line of thoughts, we hypothesized that in the presence of an oxophilic additive, a transient species derived from coordination with the 7-OH group might suffice for this purpose. The results of our studies are shown in Table 2. Of the additives examined, alkyl borate reagents consistently produced high level of diastereoselectivity (Table 2, Entries 6–16). Generation of an alkoxy anion upon deprotonation of the alcohol **17** with NaH was intended to form a more tightly bound substrate/borate complex, but the beneficial effect was modest (Table 2, Entries 7–11). Overall, use of a small borate reagent [( $\text{MeO}$ )<sub>3</sub>B] gave higher levels of stereoinduction and use of five equivalents of ( $\text{MeO}$ )<sub>3</sub>B provided the highest level of diastereoselectivity (>50:1 by  $^1\text{H}$  NMR analysis), despite a slight compromise in terms of the yield of the reaction (60%, Table 2, Entry 14).

Table 2. Additive effects in the intramolecular Diels–Alder reaction of dienone **17**.

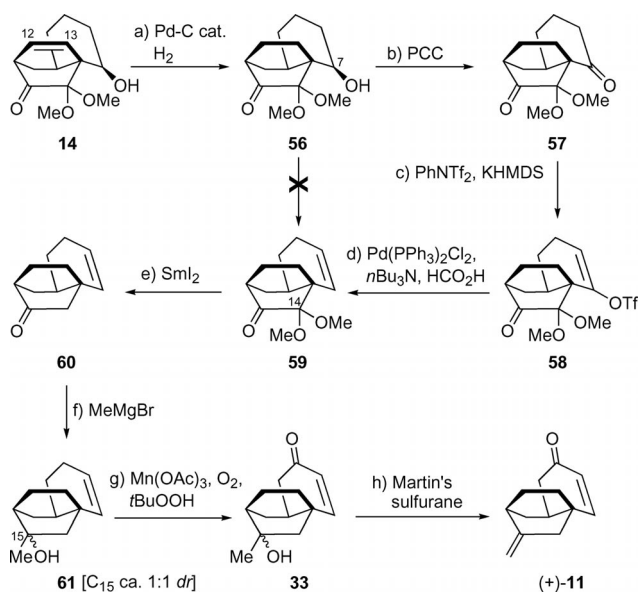
Entry <sup>[a]</sup>	Additive [equiv.]	Solvent	Yield [%] <sup>[b]</sup>	<i>dr</i> <sup>[c]</sup>
1	none	toluene	ND <sup>[d]</sup>	15:1
2	$\text{Ph}_3\text{P}$ (1.0)	toluene	ND <sup>[d]</sup>	14:1
3	TBAI/NaH (1.0)	toluene	ND <sup>[d]</sup>	14:1
4	( $\text{MeO}$ ) <sub>3</sub> B/NaH (1.0)	toluene	ND <sup>[d]</sup>	25:1
5	$\text{Ti}(\text{iPrO})_4$ (1.0)	toluene	ND <sup>[d]</sup>	20:1
6	( $\text{MeO}$ ) <sub>3</sub> B (1.0)	toluene	ND <sup>[d]</sup>	20:1
7	( $\text{MeO}$ ) <sub>3</sub> B/NaH (1.0)	toluene	23	33:1
8	( $\text{MeO}$ ) <sub>3</sub> B/NaH (3.0)	toluene	47	>50:1
9	( <i>i</i> PrO) <sub>3</sub> B/NaH (1.0)	toluene	65	17:1
10	(EtO) <sub>3</sub> B/NaH (1.0)	toluene	64	20:1
11	( $\text{MeO}$ ) <sub>3</sub> B/NaH (3.0)	toluene/THF (1:1)	62	42:1
12	( $\text{MeO}$ ) <sub>3</sub> B (1.0)	toluene	84	31:1
13	( $\text{MeO}$ ) <sub>3</sub> B (3.0)	toluene	85	31:1
14	( $\text{MeO}$ ) <sub>3</sub> B (5.0)	toluene	60	>50:1
15	( <i>i</i> PrO) <sub>3</sub> B (1.0)	toluene	63	26:1
16	(EtO) <sub>3</sub> B (1.0)	toluene	96	23:1

[a]  $\text{PhI}(\text{OAc})_2$  (1.1 equiv.),  $\text{KHCO}_3$  (2.0 equiv.), MeOH, 0 → 23 °C, 30 min; then toluene, reflux. [b] Yields refer to chromatographically and spectroscopically homogeneous materials. [c] The *dr* value was determined by  $^1\text{H}$  NMR analysis. [d] Not determined; TBAI = tetra-*n*-butylammonium iodide.

The intramolecular Diels–Alder product **14** having been secured in high diastereoisomeric and enantiomeric purity, its further elaboration to the tricyclic enone (+)-**11** was pursued next, as outlined in Scheme 6. Hydrogenation of the olefin moiety ( $\text{C}^{12}$ – $\text{C}^{13}$ ) in the tricycle **14** ( $\text{H}_2$ , Pd-C) afforded the hydroxy ketone **56** in quantitative yield. Direct elimination of the  $\text{C}_7$  hydroxy group in **56** proved unsuccessful under a variety of reaction conditions, and so a three-step procedure involving oxidation to the ketone (PCC, **57**), enol triflate formation ( $\text{PhNTf}_2$ ,  $\text{KHMDS}$ , **58**) and reduction [ $\text{Pd}(\text{PPh}_3)_4$ ,  $\text{HCO}_2\text{H}$ ] was employed to deliver the alkenyl ketone **59** in 80% yield over the three steps. The structural and stereochemical integrity of the tricyclic structure was also unambiguously confirmed through an X-ray analysis of the diketone **57** (m.p. 65–66 °C, hexane; Figure 6).<sup>[25]</sup> Furthermore, the crystallinity of the diketone **57** enabled further enantiomeric enrichment through recrystallization.

Reductive cleavage of the dimethoxy substituents ( $\text{C}^{14}$ ) in **59** was accomplished through the action of  $\text{SmI}_2$  (99% yield),<sup>[15]</sup> followed by methyl Grignard addition to the resulting ketone **60** to afford the tertiary alcohol **61**, inconsequentially as a mixture of diastereoisomers (87% yield,  $\text{C}^{15}$ : *dr* ≈ 1:1). Allylic oxidation of the olefin **61** through the action of  $\text{Mn}(\text{OAc})_3$  and *t*BuOOH<sup>[26]</sup> smoothly furnished the enone **33** (80% yield) and, finally, dehydration of the tertiary alcohol **33** (Martin's sulfurane,<sup>[17]</sup> 90% yield) completed the third-generation synthesis of the tricyclic enone core of platencin.  $^1\text{H}$  and  $^{13}\text{C}$  NMR analysis of the tricyclic enone (+)-**11**, together with optical rotation measurements, confirmed the diastereoisomeric and enantiomeric purity of the synthetic material.<sup>[9]</sup>

Completion of the total synthesis of (–)-platencin [(–)-**2**] from the tricyclic enone (+)-**11** was accomplished in accordance with the protocols developed by Nicolaou and co-



Scheme 6. Completion of the third-generation synthesis of enone (+)-11. Reagents and conditions: a) Pd-C (0.25 equiv.), H<sub>2</sub>, MeOH, 23 °C, 30 min, 100%; b) PCC (1.6 equiv.), CH<sub>2</sub>Cl<sub>2</sub>, 23 °C, 16 h, 97%; c) PhNTf<sub>2</sub> (1.4 equiv.), KHMDS (0.5 M in toluene, 2.3 equiv.), THF, -78 → 0 °C, 30 min; d) Pd(PPh<sub>3</sub>)<sub>2</sub>Cl<sub>2</sub> (0.36 equiv.), nBu<sub>3</sub>N (2.7 equiv.), HCO<sub>2</sub>H (1.8 equiv.), DMF, 70 °C, 16 h, 82% for the two steps; e) SmI<sub>2</sub> (0.1 M in THF, 4.0 equiv.), THF/MeOH (20:1), 23 °C, 15 min, 99%; f) MeMgBr (1.0 M in THF, 2.0 equiv.), THF, 0 → 23 °C, 30 min, 87% (ca. 1:1 mixture of diastereoisomers by <sup>1</sup>H NMR); g) Mn(OAc)<sub>3</sub> (0.35 equiv.), tBuOOH (5.0 M in decane, 4.8 equiv.), O<sub>2</sub>, EtOAc, 23 °C, 16 h, 80%; h) Martin's sulfurane (2.0 equiv.), CH<sub>2</sub>Cl<sub>2</sub>, 23 °C, 2 h, 90%. Tf = trifluoromethanesulfonyl, KHMDS = potassium hexamethylsilylazide, DMF = *N,N'*-dimethylformamide.

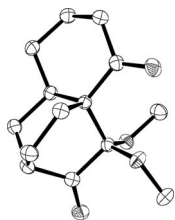
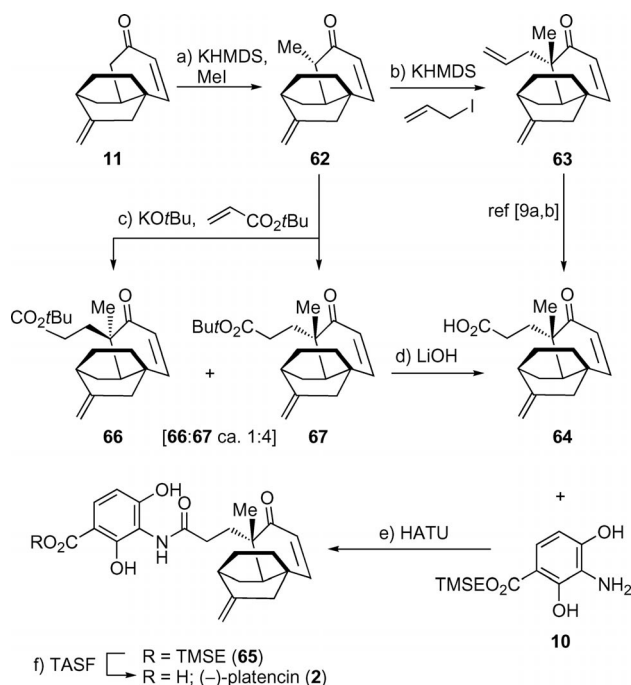


Figure 6. X-ray derived ORTEP diagram of the diketone **57** with thermal ellipsoids shown at the 50% probability level.<sup>[25]</sup>

workers (Scheme 7).<sup>[9a,9b]</sup> Sequential alkylation of the enone (+)-11 with MeI and allyl iodide afforded the terminal alkene **63** (41% yield for the two steps), which was further elaborated to the acid **64**, and coupling of this with aniline **10**<sup>[8k,9a,9b]</sup> (HATU,<sup>[27]</sup> 52% yield), followed by final deprotection (TASF,<sup>[28]</sup> 90% yield), afforded (-)-platencin [(-)-2]. Alternatively, the acid **64** could be accessed through a 1,4-addition of the enone (+)-11 to *tert*-butyl acrylate (KOtBu, *dr* ≈ 4:1),<sup>[9b,9i]</sup> followed by chromatographic separation of the two diastereoisomers (**66** and **67**) and saponification (LiOH) of the major isomer **67**. It is interesting to note that the choice of *tert*-butyl acrylate and a *t*BuOH solution of KOtBu were extremely crucial for the success of the 1,4-addition reaction.

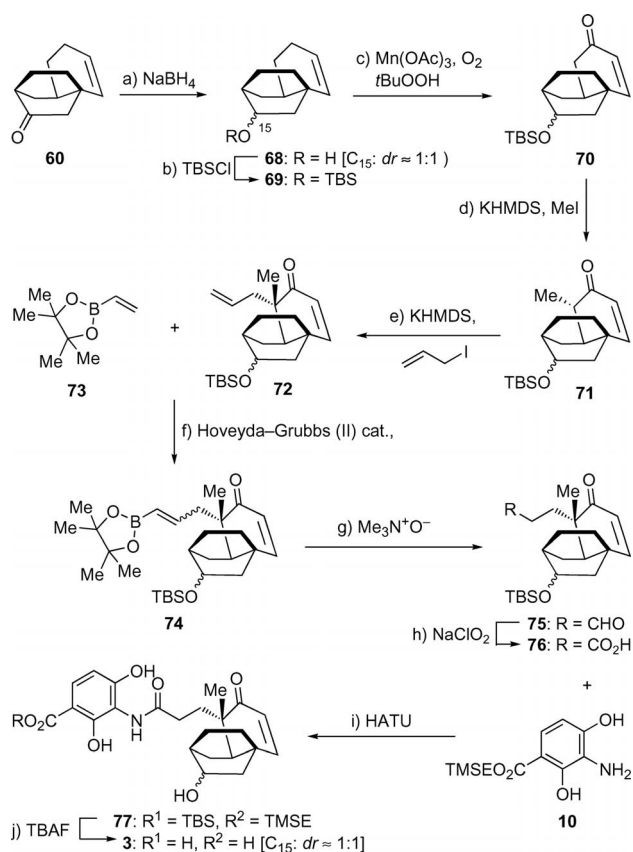


Scheme 7. Completion of the total synthesis of (-)-platencin [(-)-2]. Reagents and conditions: a) KHMDS (0.5 M in toluene, 1.1 equiv.), MeI (8.0 equiv.), THF/HMPA (4:1), -78 → 0 °C, 2 h, 61%; b) KHMDS (0.5 M in toluene, 4.0 equiv.), allyl iodide (8.0 equiv.), THF/HMPA (4:1), -78 → 0 °C, 3 h, 68%; c) *tert*-butyl acrylate (2.0 equiv.), *t*BuOK (1.0 M in *t*BuOH, 2.0 equiv.), THF, 23 °C, 20 min, 74% (ca. 4:1 mixture of diastereoisomers by <sup>1</sup>H NMR); d) LiOH (1.0 M aq., 10 equiv.), MeOH, 50 °C, 5 h; e) **10** (3.2 equiv.), HATU (3.2 equiv.), Et<sub>3</sub>N (4.2 equiv.), DMF, 23 °C, 14 h, 52% for the two steps; f) TASF (2.0 equiv.), DMF, 40 °C, 40 min, 90%. HMPA = hexamethylphosphoramide, HATU = *O*-(7-azabenzotriazol-1-yl)-1,1,3,3-tetramethyluronium hexafluorophosphate, TASF = tris(dimethylamino)sulfonium difluorotrimethylsilylate.

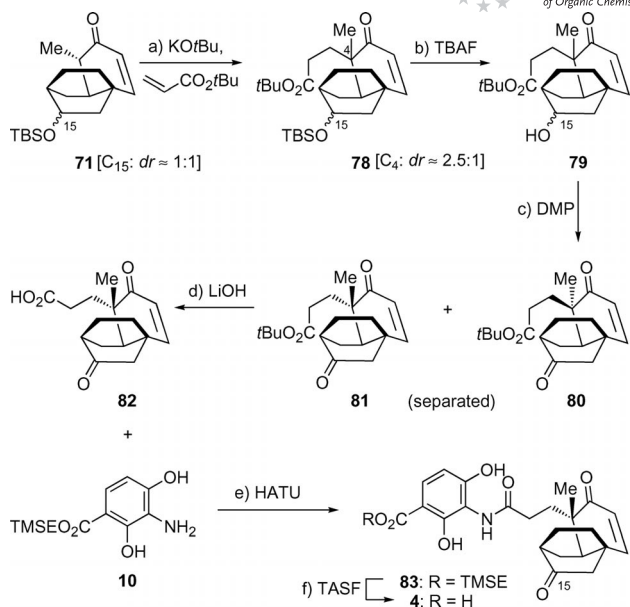
### Synthesis of Platencin Analogues

The utility of the intramolecular Diels–Alder reaction in the stereoselective construction of the highly functionalized tricyclic compound **14** having been demonstrated (Scheme 5), its application in the synthesis of analogues for chemical biology investigations was pursued next. As alluded to in the Introduction, our design of analogues was based on the molecular docking model put forward to explain the observed FabF/FabH selectivity between platensimycin (**1**) and platencin (**2**).<sup>[7b]</sup> Therefore, in addition to the total synthesis of (-)-platencin [(-)-2], the analogues **3** and **4** were synthesized as shown in Scheme 8 and Scheme 9, respectively. The synthesis of the hydroxy analogue **3** began with a NaBH<sub>4</sub> reduction of the ketone **60** to afford a ca. 1:1 mixture of the diastereoisomeric alcohols **68** in 95% yield. Silyl protection of the alcohols **68** (TBSCl), followed by allylic oxidation [Mn(OAc)<sub>3</sub>, *t*BuOOH],<sup>[26]</sup> afforded the enones **70** in 57% yield over the two steps. Sequential alkylation of the enones **70** with MeI and allyl iodide proceeded with exclusive diastereoselectivity to give the terminal olefins **72** (37% yield

over the two steps), which were subjected to olefin cross metathesis with the vinyl boronate **73**<sup>[29]</sup> in the presence of the Hoveyda–Grubbs (II) catalyst<sup>[30]</sup> to afford the vinyl boronates **74** in 57% yield. Oxidation of the vinyl boronates **74** with  $\text{Me}_3\text{N}^+\text{O}^-$  (70% yield),<sup>[31]</sup> followed by further oxidation of the resulting aldehydes **75** ( $\text{NaClO}_2$ ), afforded the acids **76**, ready for amide bond formation to attach the aromatic domain. In accordance with the conditions employed in the synthesis of (–)-platencin [(–)-**2**], HATU-mediated<sup>[27]</sup> peptide coupling between the acids **76** and the aniline **10**<sup>[8k,9a,9b]</sup> (54% from **75**), and subsequent removal of the silyl protecting groups from the amides **77** (TASF,<sup>[28]</sup> 64% yield) completed the synthesis of the hydroxy analogue **3** as a mixture of  $\text{C}^{15}$  epimers (ca. 1:1).



Scheme 8. Synthesis of the hydroxy platencin analogue **3**. Reagents and conditions: a)  $\text{NaBH}_4$  (1.2 equiv.), MeOH,  $0 \rightarrow 23^\circ\text{C}$ , 1 h, 95% (ca. 1:1 mixture of diastereoisomers by  $^1\text{H}$  NMR); b) TBSCl (1.5 equiv.), imidazole (4.0 equiv.), 4-DMAP (0.1 equiv.),  $\text{CH}_2\text{Cl}_2$ ,  $0 \rightarrow 23^\circ\text{C}$ , 16 h, 87%; c)  $\text{Mn}(\text{OAc})_3$  (0.35 equiv.),  $t\text{BuOOH}$  (5.0 m in decane, 4.8 equiv.),  $\text{O}_2$ , EtOAc,  $23^\circ\text{C}$ , 16 h, 65%; d) KHMDS (0.5 m in toluene, 1.3 equiv.), MeI (8.0 equiv.), THF/HMPA (4:1),  $-78 \rightarrow 0^\circ\text{C}$ , 2 h, 61%; e) KHMDS (0.5 m in toluene, 1.3 equiv.), allyl iodide (8.0 equiv.), THF/HMPA (4:1),  $-78 \rightarrow 0^\circ\text{C}$ , 4 h, 61%; f) **73** (5.0 equiv.), Hoveyda–Grubbs II cat. (0.1 equiv.), benzoquinone (0.1 equiv.), benzene,  $70^\circ\text{C}$ , 1 h, 57%; g)  $\text{Me}_3\text{N}^+\text{O}^-$  (5.0 equiv.), THF,  $70^\circ\text{C}$ , 3 h, 70%; h)  $\text{NaClO}_2$  (4.0 equiv.),  $\text{NaH}_2\text{PO}_4$  (7.0 equiv.), 2-methylbut-2-ene (16 equiv.),  $t\text{BuOH}/\text{H}_2\text{O}$  (1:1),  $23^\circ\text{C}$ , 90 min; i) **10** (3.0 equiv.), HATU (3.0 equiv.),  $\text{Et}_3\text{N}$  (5.7 equiv.), DMF,  $23^\circ\text{C}$ , 14 h, 54% for the two steps; j) TBAF (1.0 m in THF, 9.0 equiv.), THF,  $23^\circ\text{C}$ , 1 h, 64%. 4-DMAP =  $N,N'$ -dimethylaminopyridine.



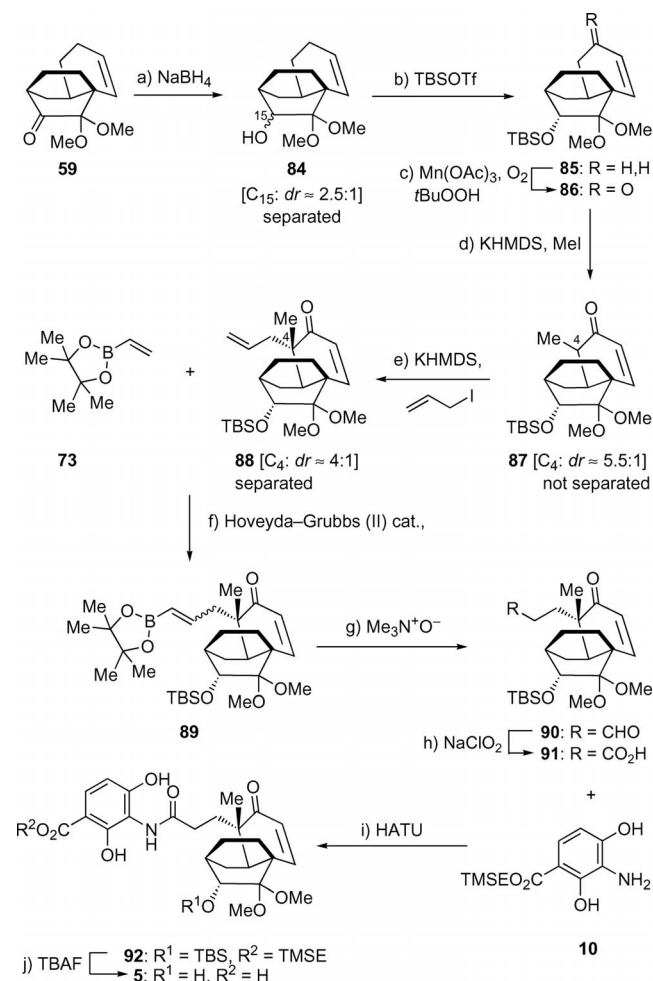
Scheme 9. Synthesis of the keto platencin analogue **4**. Reagents and conditions: a) *tert*-butyl acrylate (2.0 equiv.),  $t\text{BuOK}$  (1.0 m in  $t\text{BuOH}$ , 2.0 equiv.), THF,  $23^\circ\text{C}$ , 20 min (ca. 2.5:1 mixture of diastereoisomers by  $^1\text{H}$  NMR); b) TBAF (1.0 m in THF, 1.0 equiv.), THF,  $23^\circ\text{C}$ , 2 h; c) DMP (1.0 equiv.),  $\text{NaHCO}_3$  (1.2 equiv.),  $\text{CH}_2\text{Cl}_2$ ,  $23^\circ\text{C}$ , 2 h, 51% for the three steps; d) LiOH (1.0 m aq., 13 equiv.), MeOH,  $50^\circ\text{C}$ , 5 h; e) **10** (2.0 equiv.), HATU (2.3 equiv.),  $\text{Et}_3\text{N}$  (3.5 equiv.), DMF,  $23^\circ\text{C}$ , 14 h, 44% for the two steps; f) TASF (2.0 equiv.), DMF,  $40^\circ\text{C}$ , 80 min, 92%.

The synthesis of the analogue **4** containing a  $\text{C}^{15}$  keto moiety commenced with a 1,4-addition of the enones **71** ( $\text{C}^{15}$ :  $dr \approx 1:1$ ) to *tert*-butyl acrylate, giving the *tert*-butyl esters **78** as a ca. 2.5:1 mixture of  $\text{C}^4$  epimers (Scheme 9). Desilylation of the TBS ethers **78** (TBAF), followed by oxidation of the resulting secondary alcohols **79** (DMP), afforded a chromatographically separable mixture of the diastereoisomeric ketones **80** and **81** in 51% overall yield from the enones **71**. With stereoisomerically pure *tert*-butyl ester **81** to hand, the final steps leading to the keto analogue **4** involved an ester hydrolysis (LiOH), followed by amide coupling of the resulting carboxylic acid **82** with the aniline **10**<sup>[8k,9a,9b]</sup> (HATU)<sup>[27]</sup> and silyl deprotection (TASF)<sup>[28]</sup> to furnish the keto analogue **4** in 40% yield over the three steps.

Upon revisiting our synthetic sequence leading towards the tricyclic enone **11**, we also became interested in compounds bearing the  $\text{C}^{14}$  dimethoxy substituents for further structural diversity. In an analogous fashion, compounds bearing hydroxy, ketone and methylene functionalities at the  $\text{C}^{15}$  position, as represented by compounds **5**, **6** and **7** (Figure 1), were also synthesized, as shown in Schemes 10, 11 and 12, below, respectively.

Synthesis of hydroxy analogues such as **5** commenced with a  $\text{NaBH}_4$  reduction of the ketone **59** to afford a chromatographically separable mixture of secondary alcohols ( $dr \approx 2.5:1$ ), the major isomer of which [ $\text{C}^{15}$  stereochemistry established by X-ray crystallographic analysis of a later intermediate (**86**)] was subsequently silylated (TBSOTf) to

give the TBS ether **85** in 73% yield over the two steps (Scheme 10). Allylic oxidation of the alkene **85** [ $\text{Mn}(\text{OAc})_3$ ,  $t\text{BuOOH}$ ,<sup>[26]</sup> 53% yield] afforded the enone **86** [m.p. 86–88 °C (hexane)], the structure was confirmed by X-ray crystallographic analysis, see Figure 7,<sup>[32]</sup> and conversion of this compound into the terminal olefin **88** was by the previously described, sequential stereoselective alkylation with MeI and allyl iodide in the presence of KHMDS and HMPA (38% yield for the two steps). The terminal alkene **88** was further homologated to the vinyl boronate **89** in a fashion analogous to that described earlier for the conver-



Scheme 10. Synthesis of the dimethoxy hydroxy platencin analogue **5**. Reagents and conditions: a)  $\text{NaBH}_4$  (1.6 equiv.), MeOH, 0 °C, 1 h, 82% (ca. 2.5:1 mixture of diastereoisomers by <sup>1</sup>H NMR); b) TBSOTf (1.6 equiv.), 2,6-lutidine (2.0 equiv.),  $\text{CH}_2\text{Cl}_2$ , -78 °C, 2 h, 89%; c)  $\text{Mn}(\text{OAc})_3$  (0.35 equiv.),  $t\text{BuOOH}$  (5.0 m in decane, 4.8 equiv.),  $\text{O}_2$ , EtOAc, 23 °C, 15 h, 53%; d) KHMDS (0.5 m in toluene, 1.2 equiv.), MeI (8.0 equiv.), THF/HMPA (4:1), -78 → 0 °C, 2 h, 80% (ca. 5.5:1 mixture of diastereoisomers by <sup>1</sup>H NMR); e) KHMDS (0.5 m in toluene, 1.2 equiv.), allyl iodide (8.0 equiv.), THF/HMPA (4:1), -78 → 0 °C, 4 h, 48% (ca. 4:1 mixture of diastereoisomers by <sup>1</sup>H NMR); f) **73** (5.0 equiv.), Hoveyda-Grubbs II cat. (0.1 equiv.), benzoquinone (0.1 equiv.), benzene, 70 °C, 1 h, 35%; g)  $\text{Me}_3\text{N}^+\text{O}^-$  (5.0 equiv.), THF, 70 °C, 18 h, 100%; h)  $\text{NaClO}_2$  (3.0 equiv.),  $\text{NaH}_2\text{PO}_4$  (5.0 equiv.), 2-methylbut-2-ene (11 equiv.),  $t\text{BuOH}/\text{H}_2\text{O}$  (1:1), 23 °C, 90 min; i) **10** (3.0 equiv.), HATU (3.0 equiv.),  $\text{Et}_3\text{N}$  (4.0 equiv.), DMF, 23 °C, 14 h, 44% for the two steps; j) TBAF (1.0 m in THF, 8.0 equiv.), THF, 23 °C, 1 h, 88%.

sion from **72** to **74** (Scheme 8). Oxidation of the vinyl boronate **89** with  $\text{Me}_3\text{N}^+\text{O}^-$  (100% yield)<sup>[31]</sup> and further oxidation of the resulting aldehyde (**90**) with  $\text{NaClO}_2$  delivered the acid **91**, which was coupled with the aniline **10**<sup>[8k,9a,9b]</sup> (HATU)<sup>[27]</sup> and desilylated (TASF)<sup>[28]</sup> to complete the dimethoxy hydroxy analogue **5** (39% yield from aldehyde **90**).

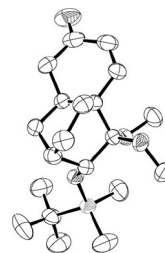
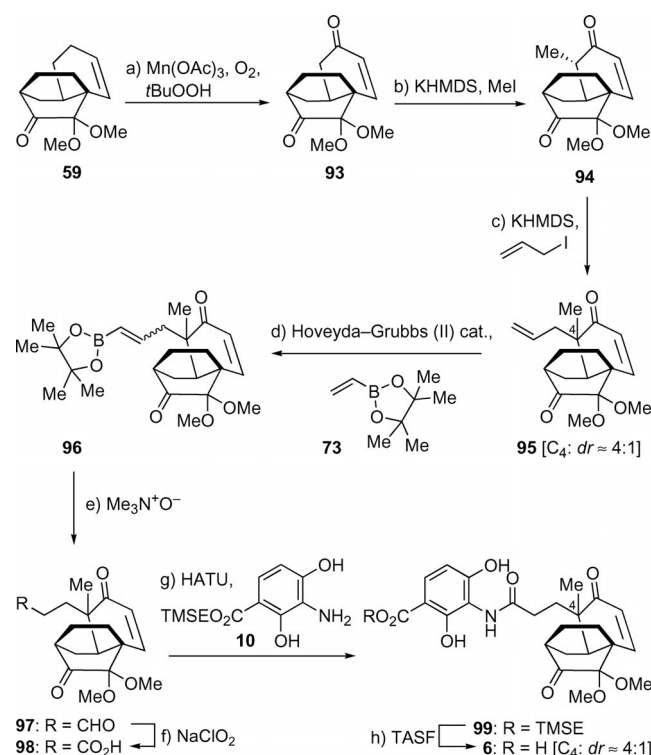


Figure 7. X-ray derived ORTEP diagram of the diketone **86** with thermal ellipsoids shown at the 50% probability level.<sup>[32]</sup>

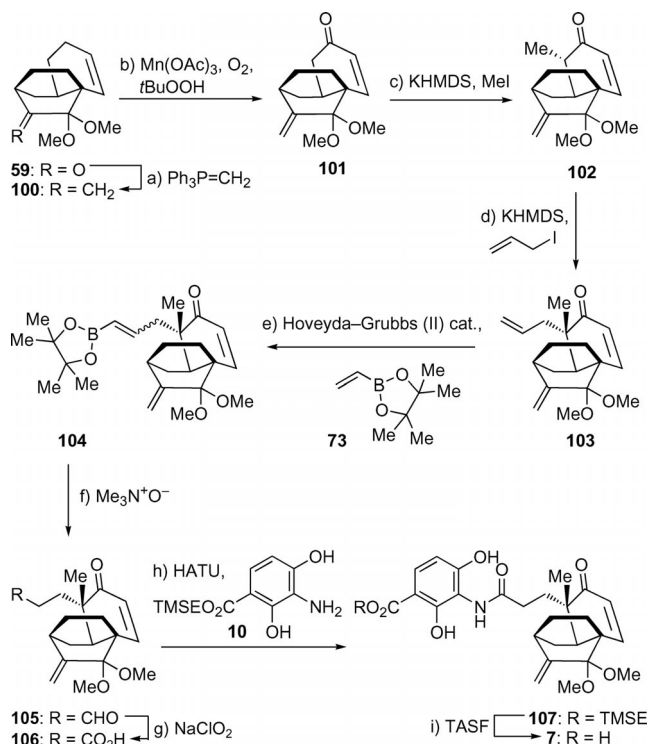
As shown in Scheme 11, the synthesis of the dimethoxy ketone analogue **6** took advantage of the dimethoxy ketone **59**, and its conversion into the enone **93** was carried out by



Scheme 11. Synthesis of the dimethoxy ketone platencin analogue **6**. Reagents and conditions: a)  $\text{Mn}(\text{OAc})_3$  (0.35 equiv.),  $t\text{BuOOH}$  (5.0 m in decane, 4.8 equiv.),  $\text{O}_2$ , EtOAc, 23 °C, 16 h, 73%; b) KHMDS (0.5 m in toluene, 1.2 equiv.), MeI (8.0 equiv.), THF/HMPA (4:1), -78 → 0 °C, 2 h, 72%; c) KHMDS (0.5 m in toluene, 1.2 equiv.), allyl iodide (8.0 equiv.), THF/HMPA (4:1), -78 → 0 °C, 4 h, 56% (ca. 4:1 mixture of diastereoisomers by <sup>1</sup>H NMR); d) **73** (5.0 equiv.), Hoveyda-Grubbs II cat. (0.1 equiv.), benzoquinone (0.1 equiv.), benzene, 70 °C, 1 h, 35%; e)  $\text{Me}_3\text{N}^+\text{O}^-$  (5.0 equiv.), THF, 70 °C, 3 h, 74%; f)  $\text{NaClO}_2$  (3.0 equiv.),  $\text{NaH}_2\text{PO}_4$  (5.0 equiv.), 2-methylbut-2-ene (11 equiv.),  $t\text{BuOH}/\text{H}_2\text{O}$  (1:1), 23 °C, 90 min; g) **10** (3.0 equiv.), HATU (3.0 equiv.),  $\text{Et}_3\text{N}$  (4.0 equiv.), DMF, 23 °C, 14 h, 60% for the two steps; h) TASF (2.0 equiv.), DMF, 40 °C, 80 min, 81%.

the  $\text{Mn}(\text{OAc})_3/t\text{BuOOH}$  protocol<sup>[26]</sup> in 73% yield. Sequential alkylation of the enone **93** with MeI and allyl iodide led to an inseparable pair of diastereoisomers epimeric at C<sup>4</sup> (**95**, *dr*  $\approx$  4:1), which were further elaborated to the acid **98** through the cross-metathesis and double oxidation sequence. Amide bond coupling between the acid **98** and the aniline **10**<sup>[8k,9a,9b]</sup> (HATU)<sup>[27]</sup> and final deprotection (TASF)<sup>[28]</sup> then completed the dimethoxy ketone analogue **6** in 49% yield from **97** (*dr*  $\approx$  4:1).

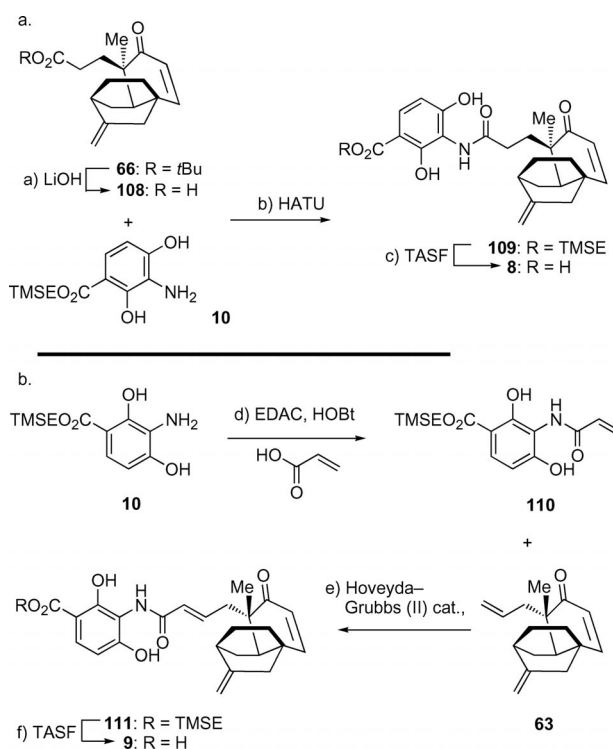
The synthesis of the dimethoxy methylene analogue **7** began with a Wittig olefination of the ketone **59** ( $\text{Ph}_3\text{P}=\text{CH}_2$ , **100**), followed by allylic oxidation [ $\text{Mn}(\text{OAc})_3$ ,  $t\text{BuOOH}$ ]<sup>[26]</sup> to afford the enone **101** in 64% yield over the two steps (Scheme 12). The double alkylation product **103** was obtained as a single diastereoisomer under the previously described conditions (46% yield over the two steps from the enone **101**). Olefin cross-metathesis (**73**,<sup>[29]</sup> Hoveyda–Grubbs II catalyst)<sup>[30]</sup> and subsequent oxidations



Scheme 12. Synthesis of the dimethoxy methylene platencin analogue **7**. Reagents and conditions: a) (bromomethyl)triphenylphosphonium bromide (8.0 equiv.),  $t\text{BuONa}$  (8.0 equiv.),  $\text{Et}_2\text{O}$ , 45 °C, 2 h, 80%; b)  $\text{Mn}(\text{OAc})_3$  (0.35 equiv.),  $t\text{BuOOH}$  (5.0 M in decane, 4.8 equiv.),  $\text{O}_2$ ,  $\text{EtOAc}$ , 23 °C, 15 h, 80%; c) KHMDS (0.5 M in toluene, 1.2 equiv.), MeI (8.0 equiv.), THF/HMPA (4:1),  $-78 \rightarrow 0$  °C, 2 h, 76%; d) KHMDS (0.5 M in toluene, 1.2 equiv.), allyl iodide (8.0 equiv.), THF/HMPA (4:1),  $-78 \rightarrow 0$  °C, 4 h, 60%; e) **73** (5.0 equiv.), Hoveyda–Grubbs II cat. (0.1 equiv.), benzoquinone (0.1 equiv.), benzene, 70 °C, 1 h, 65%; f)  $\text{Me}_3\text{N}^+\text{O}^-$  (5.0 equiv.), THF, 70 °C, 3 h, 60%; g)  $\text{NaClO}_2$  (7.0 equiv.), 2-methylbut-2-ene (15 equiv.),  $t\text{BuOH}/\text{H}_2\text{O}$  (1:1), 23 °C, 90 min; h) **10** (3.0 equiv.), HATU (3.0 equiv.),  $\text{Et}_3\text{N}$  (5.0 equiv.), DMF, 23 °C, 14 h, 63% for the two steps; i) TASF (2.0 equiv.), DMF, 40 °C, 80 min, 47%.

( $\text{Me}_3\text{N}^+\text{O}^-$  then  $\text{NaClO}_2$ )<sup>[31]</sup> of the intermediate vinyl boronate **104** proceeded uneventfully to deliver the acid **106**, amide coupling of which (HATU)<sup>[27]</sup> with the aniline **10** and final deprotection (TASF)<sup>[28]</sup> gave the dimethoxy methylene analogue **7** in 30% yield from the aldehyde **105**.

As the final additions to our collection of platencin analogues, the reverse alkylation analogue **8** [C<sup>4</sup>-*epi*-platencin, C<sup>4</sup>-*epi*-(-)-**2**] and the  $\alpha,\beta$ -unsaturated amide **9** were also synthesized, as shown in Scheme 13. Hydrolysis (LiOH) of the previously described diastereoisomeric *tert*-butyl ester **66** (Scheme 7), followed by amide coupling with the aniline **10**<sup>[8k,9a,9b]</sup> (HATU)<sup>[27]</sup> and desilylation (TASF)<sup>[28]</sup> furnished C<sup>4</sup>-*epi*-platencin (**8**) in 48% yield over the three steps (Scheme 13, a).



Scheme 13. Syntheses of the reverse-alkylation platencin analogue **8** and the  $\alpha,\beta$ -unsaturated amide **9**. Reagents and conditions: a) LiOH (1.0 M aq., 10 equiv.), MeOH, 50 °C, 5 h; b) **10** (2.2 equiv.), HATU (2.2 equiv.),  $\text{Et}_3\text{N}$  (3.2 equiv.), DMF, 23 °C, 14 h, 57% for the two steps; c) TASF (1.4 equiv.), 40 °C, 80 min, 85%; d) acrylic acid (1.0 equiv.),  $\text{Et}_3\text{N}$  (1.3 equiv.), HOBT (1.0 equiv.), EDAC (1.0 equiv.), DMF, 23 °C, 16 h, 94%; e) **110** (1.3 equiv.), Hoveyda–Grubbs II cat. (0.05 equiv.),  $\text{CH}_2\text{Cl}_2$ , 50 °C, 12 h, 42%; f) TASF (2.0 equiv.), DMF, 40 °C, 80 min, 95%. HOBT = *N*-hydroxybenzotriazole, EDAC = 1-ethyl-3-(3-dimethylaminopropyl)carbodiimide.

Olefin cross-metathesis with the terminal alkene **63** and the acrylamide **110** in the presence of the Hoveyda–Grubbs II catalyst<sup>[30]</sup> smoothly delivered the  $\alpha,\beta$ -unsaturated amide **111** as a single geometric isomer, which was desilylated (TASF)<sup>[28]</sup> to give the analogue **9** in 40% overall yield for the two steps (Scheme 13, b).

Table 3. Antibacterial studies of (–)-platencin [(–)-2] and its analogues 3–9.

Entry		MIC <sup>[a]</sup> [ $\mu\text{g/mL}$ ]	<i>S. aureus</i> Mu50 (VISA)	<i>S. aureus</i> ATCC43300 (MRSA)	<i>B. subtilis</i> 168	<i>S. aureus</i> SG511	<i>E. coli</i> W3110	<i>P. aeruginosa</i> PA01
		<i>S. aureus</i> COL (MRSA)						
1	(–)-2	0.1	0.25	0.25	0.5	0.25	>128	>128
2	3	>128	>128	>128	>128	>128	>128	>128
3	4	>128	>128	>128	>128	>128	>128	>128
4	5	16	32	64	>128	>128	>128	>128
5	6	8	16	16	>128	8	>128	>128
6	7	4	8	8	>128	32	>128	>128
7	8	8	1	1	2	1	>128	>128
8	9	>128	>128	>128	>128	>128	>128	>128

[a] Minimal inhibitory concentrations (MICs) were determined by a standard microtitre plate assay. Compound stock solutions ( $10 \text{ mg mL}^{-1}$ ) were prepared in DMSO. Serial dilutions of compounds in Luria Bertani (LB) broth were inoculated with  $5 \times 10^5 \text{ cells mL}^{-1}$  and incubated for 18 h at  $37^\circ\text{C}$ .

### Antibacterial Studies of (–)-Platencin [(–)-2] and the Platencin Analogues 3–9

The synthesized compounds were tested against a panel of bacterial strains, including *S. aureus* COL (MRSA), *S. aureus* Mu50 (VISA), *S. aureus* ATCC43300 (MRSA), *B. subtilis* 168, *S. aureus* SG511, *E. coli* W3110 and *P. aeruginosa* PA01 with synthetic (–)-platencin [(–)-2] as positive control, and the results are summarized in Table 3. The hydroxy analogue 3 (Table 3, Entry 2) and the ketone analogue 4 (Table 3, Entry 3) of platencin showed complete loss of antibacterial activities against both normal and resistant strains. The dimethoxy analogues 5–7 (Table 3, Entries 4–6) also showed significant reduction in antibacterial activities, but these compounds seem to show selectivity toward the resistant strains *S. aureus* COL (MRSA), *S. aureus* Mu50 (VISA), *S. aureus* ATCC43300 (MRSA) and *S. aureus* SG511. Much to our surprise, the reverse alkylation analogue 8 also showed modest levels of antibiotic activity, whereas the  $\alpha,\beta$ -unsaturated amide 9 showed complete loss of antibacterial activities. Clearly, further studies are needed in order to seek structural simplification and diversification in parallel with improvement of platencin's antibiotic property. Work in this area, together with the FabF/FabH selectivity of analogues 3–9, is currently underway and the results will be reported in due course.

### Conclusions

In summary, the total synthesis of the recently disclosed, broad-spectrum fatty-acid synthase inhibitory antibiotic (–)-platencin [(–)-2] has been accomplished. The synthetic strategy featured the application of the masked *o*-benzoquinones intramolecular Diels–Alder reaction, and highlighted the directing effect of remote stereocentres in the alkenyl side chain, as illustrated in substrates 15, 16, and 17, in the observed diastereoselectivity of the intramolecular Diels–Alder reaction. Furthermore, the use of borate reagent as an additive led to dramatic improvements in the diastereoselectivity of the Diels–Alder reaction of substrate 17. The developed synthetic strategy, together with the readily accessible and highly functionalized tricyclic system 14, facili-

tated the preparation of rationally designed analogues incorporating hydrogen bond donating, accepting and lipophilic substituents at  $\text{C}^{15}$ , as demonstrated in the synthesis of the platencin analogues 3–9. The highly flexible synthetic technology, together with preliminary SAR insights, should enable further chemical biology investigations of this fascinating class of compounds.

**Supporting Information** (see also the footnote on the first page of this article): General information for the Experimental Section, experimental procedures and compound characterization, materials and methods for antibacterial assays, and  $^1\text{H}$  and  $^{13}\text{C}$  NMR spectra for all compounds.

### Acknowledgments

We thank Ms. Sanny G. Ing (ICES-CSL), Mr. Kelvin S.-L. Chan (ICES-CSL), and Ms. Catherine Lau (ICES-CSL) for their assistance, Dr. Aitipamula Srinivasulu (ICES) and Ms. Chia Sze Chen (ICES) for X-ray crystallographic analysis, and Ms. Doris Tan (ICES) for high-resolution mass spectrometric (HRMS) assistance. Financial support for this work was provided by A\*STAR, Singapore.

- [1] a) G. S. Omenn, *Proc. Natl. Acad. Sci. USA* **2010**, *107*, 1702–1709; b) K. E. Jones, N. G. Patel, M. A. Levy, A. Storeygard, D. Balk, J. L. Gittleman, P. Daszak, *Nature* **2008**, *451*, 990–993.
- [2] a) J. Davies, *Antibiotic Resistance: Origins, Evolution, Selection and Spread*, Wiley, **1997**. For a series of reviews on antibiotic resistance, see: ; b) C. T. Walsh, G. Wright, *Chem. Rev.* **2005**, *105*, 391–774; c) K. M. Overbye, J. F. Barrett, *Drug Disc. Today* **2005**, *10*, 45–52.
- [3] a) M. A. Fischbach, C. T. Walsh, *Science* **2009**, *325*, 1089–1093; b) A. L. Demain, S. Sanchez, *J. Antibiot.* **2009**, *62*, 5–16; c) M. Gualtieri, F. Baneres-Roquet, P. Villain-Guillot, M. Pugniere, J.-P. Leonetti, *Curr. Med. Chem.* **2009**, *16*, 390–393; d) D. J. Payne, M. N. Gwynn, D. J. Holmes, D. L. Pompliano, *Nat. Rev. Drug Discovery* **2007**, *6*, 29–40.
- [4] a) S. W. White, J. Zheng, Y.-M. Zhang, C. O. Rock, *Annu. Rev. Biochem.* **2005**, *74*, 791–831; b) J. W. Campbell, J. E. Cronan Jr., *Annu. Rev. Microbiol.* **2001**, *55*, 305–332; c) R. J. Heath, S. W. White, C. O. Rock, *Prog. Lipid. Res.* **2001**, *40*, 467–497; d) R. J. Heath, C. O. Rock, *Curr. Opin. Invest. Drugs* **2004**, *5*, 146–153; e) Y.-M. Zhang, Y.-J. Lu, C. O. Rock, *Lipids* **2004**, *39*, 1055–1060; f) H. T. Wright, K. A. Reynolds, *Curr. Opin. Microbiol.* **2007**, *10*, 447–453.

- [5] a) K. Young, H. Jayasuriya, J. G. Ondeyka, K. Herath, C. Zhang, S. Kodali, A. Galgoci, R. Painter, V. Brown-Driver, R. Yamamoto, L. L. Silver, Y. Zheng, J. I. Ventura, J. Sigmund, S. Ha, A. Basilio, F. Vicente, J. F. Tormo, F. Pelaez, P. Youngman, D. Cully, J. F. Barrett, D. Schmatz, S. B. Singh, J. Wang, *Antimicrob. Agents Chemother.* **2006**, *50*, 519–526; b) R. J. Heath, Y. T. Yu, M. A. Shapiro, E. Olson, C. O. Rock, *J. Biol. Chem.* **1998**, *273*, 30316–30320; c) A. Banerjee, E. Dubnau, A. Quemard, V. Balasubramanian, K. S. Um, T. Wilson, D. Collins, G. de Lisle, W. R. Jacobs Jr., *Science* **1994**, *263*, 227–230; d) C. Baldock, J. B. Rafferty, S. E. Sedelnikova, P. J. Baker, A. R. Stuitje, A. R. Slabas, T. R. Hawkes, D. W. Rice, *Science* **1999**, *274*, 2107–2110; e) D. A. Heerding, G. Chan, W. E. DeWolf, A. P. Fosberry, C. A. Janson, D. D. Jaworski, E. McManus, W. H. Miller, T. D. Moore, D. J. Payne, X. Qiu, S. F. Rittenhouse, C. Slater-Radosti, W. Smith, D. T. Takata, K. S. Vaidya, C. C. Yuan, W. F. Huffman, *Bioorg. Med. Chem. Lett.* **2001**, *11*, 2061–2065; f) M. A. Seefeld, W. H. Miller, K. A. Newlander, W. J. Burgess, W. E. DeWolf, Jr., P. A. Elkins, M. A. Head, D. R. Jakas, C. A. Janson, P. M. Keller, P. J. Manley, T. D. Moore, D. J. Paine, S. Pearson, B. J. Polizzi, X. Qiu, S. F. Rittenhouse, I. N. Uzinskas, N. G. Wallis, W. F. Huffman, *J. Med. Chem.* **2003**, *46*, 1627–1635; g) A. C. Price, K. H. Choi, R. J. Heath, Z. Li, S. W. White, C. O. Rock, *J. Biol. Chem.* **2001**, *276*, 6551–6559; h) C. Freiberg, N. A. Brunner, G. Schiffer, T. Lampe, J. Pohlmann, M. Brands, M. Raabe, D. Häbich, K. Ziegelbauer, *J. Biol. Chem.* **2004**, *279*, 26066–26073.
- [6] For isolation of platensimycin, see: a) J. Wang, S. M. Soisson, K. Young, W. Shoop, S. Kodali, A. Galgoci, R. Painter, G. Parthasarathy, Y. S. Tang, R. Cummings, S. Ha, K. Dorso, M. Motyl, H. Jayasuriya, J. Ondeyka, K. Herath, C. Zhang, L. Hernandez, J. Allocco, A. Basilio, J. R. Tormo, O. Genilloud, F. Vicente, F. Pelaez, L. Colwell, S. H. Lee, B. Michael, T. Felcetto, C. Gill, L. L. Silver, J. D. Hermes, K. Bartzial, J. Barrett, D. Schmatz, J. W. Becker, D. Cully, S. B. Singh, *Nature* **2006**, *441*, 358–361; b) S. B. Singh, H. Jayasuriya, J. G. Ondeyka, K. B. Herath, C. Zhang, D. L. Zink, N. N. Tsou, R. G. Ball, A. Basilio, O. Genilloud, M. T. Diez, F. Vicente, F. Pelaez, K. Young, J. Wang, *J. Am. Chem. Soc.* **2006**, *128*, 11916–11920; c) S. B. Singh, K. B. Herath, J. Wang, N. Tsou, R. G. Ball, *Tetrahedron Lett.* **2007**, *48*, 5429–5433; d) K. B. Herath, A. B. Attygalle, S. B. Singh, *J. Am. Chem. Soc.* **2007**, *129*, 15422–15423.
- [7] For isolation of platencin, see: a) J. Wang, S. Kodali, S. H. Lee, A. Galgoci, R. Painter, K. Dorso, F. Racine, M. Motyl, L. Hernandez, E. Tinney, S. Colletti, K. Herath, R. Cummings, O. Salazar, I. Gonzalez, A. Basilio, F. Vicente, O. Genilloud, F. Pelaez, H. Jayasuriya, K. Young, D. Cully, S. B. Singh, *Proc. Natl. Acad. Sci. USA* **2007**, *104*, 7612–7616; b) H. Jayasuriya, K. B. Herath, C. Zhang, D. L. Zink, A. Basilio, O. Genilloud, M. T. Diez, F. Vicente, I. Gonzalez, O. Salazar, F. Pelaez, R. Cummings, S. Ha, J. Wang, S. B. Singh, *Angew. Chem.* **2007**, *119*, 4768–4772; *Angew. Chem. Int. Ed.* **2007**, *46*, 4684–4688.
- [8] a) K. C. Nicolaou, A. Li, D. J. Edmonds, *Angew. Chem.* **2006**, *118*, 7244–7248; *Angew. Chem. Int. Ed.* **2006**, *45*, 7086–7090; b) K. C. Nicolaou, D. J. Edmonds, A. Li, G. S. Tria, *Angew. Chem.* **2007**, *119*, 4016–4019; *Angew. Chem. Int. Ed.* **2007**, *46*, 3942–3945; c) Y. Zou, C.-H. Chen, C. D. Taylor, B. M. Foxman, B. B. Snider, *Org. Lett.* **2007**, *9*, 1825–1828; d) K. C. Nicolaou, Y. Tang, J. Wang, *Chem. Commun.* **2007**, 1922–1923; e) P. Li, J. N. Payette, H. Yamamoto, *J. Am. Chem. Soc.* **2007**, *129*, 9534–9535; f) G. Lalic, E. J. Corey, *Org. Lett.* **2007**, *9*, 4921–4923; g) K. Tiefenbacher, J. Mulzer, *Angew. Chem.* **2007**, *119*, 8220–8221; *Angew. Chem. Int. Ed.* **2007**, *46*, 8074–8075; h) K. C. Nicolaou, D. Pappo, K. Y. Tsang, R. Gibe, D. Y.-K. Chen, *Angew. Chem.* **2008**, *120*, 958–960; *Angew. Chem. Int. Ed.* **2008**, *47*, 944–946; i) C. H. Kim, K. P. Jang, S. Y. Choi, Y. K. Chung, E. Lee, *Angew. Chem.* **2008**, *120*, 4073–4075; *Angew. Chem. Int. Ed.* **2008**, *47*, 4009–4011; j) J.-I. Matsuo, K. Takeuchi, H. Ishibashi, *Org. Lett.* **2008**, *10*, 4049–4052; k) A. K. Ghosh, K. Xi, *J. Org. Chem.* **2009**, *74*, 1163–1170; l) S. Y. Yun, J.-C. Zheng, D. Lee, *J. Am. Chem. Soc.* **2009**, *131*, 8413–8415; m) K. C. Nicolaou, A. Li, S. P. Ellery, D. J. Edmonds, *Angew. Chem.* **2009**, *121*, 4411–4413; *Angew. Chem. Int. Ed.* **2009**, *48*, 6293–6295; n) N. A. McGrath, E. S. Bartlett, S. Sittihan, J. T. Njardarson, *Angew. Chem.* **2009**, *121*, 8695–8698; *Angew. Chem. Int. Ed.* **2009**, *48*, 8543–8546; o) K. C. Nicolaou, A. Li, D. J. Edmonds, G. S. Tria, S. P. Ellery, *J. Am. Chem. Soc.* **2009**, *131*, 16905–16918; p) S. Xing, W. Pan, C. Liu, J. Ren, Z. Wang, *Angew. Chem.* **2010**, *122*, 3283–3286; *Angew. Chem. Int. Ed.* **2010**, *49*, 3215–3218; q) K. Tiefenbacher, L. Troendlin, J. Mulzer, A. Pfaltz, *Tetrahedron* **2010**, *66*, 6508–6513. For studies directed toward the platensimycin core, see: r) A. K. Ghosh, K. Xi, *Org. Lett.* **2007**, *9*, 4013–4016; s) K. P. Kaliappan, V. Ravikumar, *Org. Lett.* **2007**, *9*, 2417–2419. For reviews on the synthesis of platensimycin and related antibiotics, see: t) K. C. Nicolaou, J. S. Chen, D. J. Edmonds, A. A. Estrada, *Angew. Chem.* **2009**, *121*, 670–732; *Angew. Chem. Int. Ed.* **2009**, *48*, 660–719; u) K. Tiefenbacher, J. Mulzer, *Angew. Chem.* **2008**, *120*, 2582–2590; *Angew. Chem. Int. Ed.* **2008**, *47*, 2548–2555; v) K. Palanichamy, K. P. Kaliappan, *Chem. Asian J.* **2010**, *5*, 668–703.
- [9] a) K. C. Nicolaou, G. S. Tria, D. J. Edmonds, *Angew. Chem.* **2008**, *120*, 1804–1807; *Angew. Chem. Int. Ed.* **2008**, *47*, 1780–1783; b) K. C. Nicolaou, G. S. Tria, D. J. Edmonds, M. Kar, *J. Am. Chem. Soc.* **2009**, *131*, 15909–15917; c) J. Hayashida, V. H. Rawal, *Angew. Chem.* **2008**, *120*, 4445–4448; *Angew. Chem. Int. Ed.* **2008**, *47*, 4373–4376; d) K. Tiefenbacher, J. Mulzer, *Angew. Chem.* **2008**, *120*, 6294–6295; *Angew. Chem. Int. Ed.* **2008**, *47*, 6199–6200; e) S. Y. Yun, J.-C. Zheng, D. Lee, *Angew. Chem.* **2008**, *120*, 6297–6299; *Angew. Chem. Int. Ed.* **2008**, *47*, 6201–6203; f) D. C. J. Waalboer, M. C. Schaapman, F. L. Van Delft, F. P. J. T. Rutjes, *Angew. Chem.* **2008**, *120*, 6678–6680; *Angew. Chem. Int. Ed.* **2008**, *47*, 6576–6578; g) K. C. Nicolaou, Q.-Y. Toh, D. Y.-K. Chen, *J. Am. Chem. Soc.* **2008**, *130*, 11292–11293; h) K. A. B. Austin, M. G. Banwell, A. C. Willis, *Org. Lett.* **2008**, *10*, 4465–4468; i) K. Tiefenbacher, J. Mulzer, *J. Org. Chem.* **2009**, *74*, 2937–2941; j) G. N. Varseev, M. E. Maier, *Angew. Chem.* **2009**, *121*, 3739–3742; *Angew. Chem. Int. Ed.* **2009**, *48*, 3685–3688; k) A. K. Ghosh, K. Xi, *Angew. Chem.* **2009**, *121*, 5476–5479; *Angew. Chem. Int. Ed.* **2009**, *48*, 5372–5375. For a review on the synthesis of platencin, see: l) K. Palanichamy, K. P. Kaliappan, *Chem. Asian J.* **2010**, *5*, 668–703.
- [10] a) K. C. Nicolaou, T. Lister, R. M. Denton, A. Montero, D. J. Edmonds, *Angew. Chem.* **2007**, *119*, 4796–4798; *Angew. Chem. Int. Ed.* **2007**, *46*, 4712–4714; b) K. C. Nicolaou, Y. Tang, J. Wang, A. F. Stepan, A. Li, A. Montero, *J. Am. Chem. Soc.* **2007**, *129*, 14850–14851; c) K. C. Nicolaou, A. F. Stepan, T. Lister, A. Li, A. Montero, G. S. Tria, C. I. Turner, Y. Tang, J. Wang, R. M. Denton, D. J. Edmonds, *J. Am. Chem. Soc.* **2008**, *130*, 13110–13119; d) Y.-Y. Yeung, E. J. Corey, *Org. Lett.* **2008**, *10*, 3877–3878; e) J. Wang, V. Lee, H. O. Sintim, *Chem. Eur. J.* **2009**, *15*, 2747–2750; f) H. C. Shen, F. Ding, S. B. Singh, G. Parthasarathy, S. M. Soisson, S. N. Ha, X. Chen, S. Kodali, J. Wang, K. Dorso, J. R. Tata, M. L. Hammond, M. MacCoss, S. L. Colletti, *Bioorg. Med. Chem. Lett.* **2009**, *19*, 1623–1627; g) K. P. Jang, C. H. Kim, S. W. Na, H. Kim, H. Kang, E. Lee, *Bioorg. Med. Chem. Lett.* **2009**, *19*, 4601–4602; h) O. V. Barykina, K. L. Rossi, M. J. Rybak, B. B. Snider, *Org. Lett.* **2009**, *11*, 5334–5337; i) K. Tiefenbacher, A. Gollner, J. Mulzer, *Chem. Eur. J.* **2010**, *16*, 9616–9622; j) D. C. J. Waalboer, S. H. A. M. Leenders, T. Schülin-Casonato, F. L. Van Delft, F. P. J. T. Rutjes, *Chem. Eur. J.* **2010**, *16*, 11233–11236.
- [11] K. C. Nicolaou, S. A. Snyder, T. Montagnon, G. Vassilikogianakis, *Angew. Chem.* **2002**, *114*, 1742–1773; *Angew. Chem. Int. Ed.* **2002**, *41*, 1668–1698.
- [12] Y.-K. Chen, R. K. Peddinti, C.-C. Liao, *Chem. Commun.* **2001**, *15*, 1340–1341, and references cited therein.
- [13] T. Harayama, T. Sato, Y. Nakano, H. Abe, Y. Takeuchi, *Heterocycles* **2003**, *59*, 293–301.

- [14] CCDC-781698 contains the supplementary crystallographic data for compound **29a**. These data can be obtained free of charge from The Cambridge Crystallographic Data Centre via [www.ccdc.cam.ac.uk/data\\_request/cif](http://www.ccdc.cam.ac.uk/data_request/cif).
- [15] For selected reviews on the use of samarium diiodide in chemical synthesis, see: a) K. C. Nicolaou, S. P. Ellery, J. S. Chen, *Angew. Chem.* **2009**, *121*, 7376–7301; *Angew. Chem. Int. Ed.* **2009**, *48*, 7140–7165; b) D. J. Edmonds, D. Johnston, D. J. Procter, *Chem. Rev.* **2004**, *104*, 3371–3403; c) H. B. Kagan, *Tetrahedron* **2003**, *59*, 10351–10372; d) G. A. Molander, C. R. Harris, *Chem. Rev.* **1996**, *96*, 307–338.
- [16] Y. Ito, T. Hirao, T. Saegusa, *J. Org. Chem.* **1978**, *43*, 1011–1013.
- [17] a) J. C. Martin, R. J. Arhart, *J. Am. Chem. Soc.* **1971**, *93*, 4327–4329; b) R. J. Arhart, J. C. Martin, *J. Am. Chem. Soc.* **1972**, *94*, 5003–5010.
- [18] A. B. Northrup, D. W. C. MacMillan, *J. Am. Chem. Soc.* **2002**, *124*, 6798–6799.
- [19] P. A. Grieco, S. Gilman, M. Nishizawa, *J. Org. Chem.* **1976**, *41*, 1485–1486.
- [20] a) G. M. Atkins Jr., E. M. Burgess, *J. Am. Chem. Soc.* **1968**, *90*, 4744–4745; b) E. M. Burgess, H. R. Penton Jr., E. A. Taylor, *J. Am. Chem. Soc.* **1970**, *92*, 5224–5226; c) E. M. Burgess, H. R. Penton Jr., E. A. Taylor, *J. Org. Chem.* **1973**, *38*, 26–31.
- [21] CCDC-781697 contains the supplementary crystallographic data for compound **40**. This data can be obtained free of charge from The Cambridge Crystallographic Data Centre via [www.ccdc.cam.ac.uk/data\\_request/cif](http://www.ccdc.cam.ac.uk/data_request/cif).
- [22] A. Stern, J. S. Swenton, *J. Org. Chem.* **1987**, *52*, 2763–2768.
- [23] a) S. Nahm, S. M. Weinreb, *Tetrahedron Lett.* **1981**, *22*, 3815–3818. For the Weinreb amide **49**, see: b) V. Satcharoen, N. J. McLean, S. C. Kemp, N. P. Camp, R. C. D. Brown, *Org. Lett.* **2007**, *9*, 1867–1869.
- [24] E. J. Corey, C. J. Helal, *Angew. Chem.* **1998**, *110*, 2092–2118; *Angew. Chem. Int. Ed.* **1998**, *37*, 1986–2012.
- [25] CCDC-781877 contains the supplementary crystallographic data for compound **57**. These data can be obtained free of charge from The Cambridge Crystallographic Data Centre via [www.ccdc.cam.ac.uk/data\\_request/cif](http://www.ccdc.cam.ac.uk/data_request/cif).
- [26] T. K. M. Shing, Y.-Y. Yeung, P. L. Su, *Org. Lett.* **2006**, *8*, 3149–3151.
- [27] L. Carpino, A. El-Faham, C. A. Minor, F. Albericio, *J. Chem. Soc., Chem. Commun.* **1994**, *2*, 201–203.
- [28] W. J. Middleton, *Org. Synth. Coll. Vol.* **1990**, *7*, 528.
- [29] C. Morrill, R. H. Grubbs, *J. Org. Chem.* **2003**, *68*, 6031–6034.
- [30] a) J. S. Kingsbury, J. P. A. Harrity, P. J. Bonitatebus, A. H. Hoveyda, *J. Am. Chem. Soc.* **1999**, *121*, 791–799; b) S. B. Garber, J. S. Kingsbury, B. L. Gray, A. H. Hoveyda, *J. Am. Chem. Soc.* **2000**, *122*, 8168–8179; c) For a short review on these catalysts, see: A. H. Hoveyda, D. G. Gillingham, J. J. Van Veldhuizen, O. Kataoka, S. B. Garber, J. S. Kingsbury, J. P. A. Harrity, *Org. Biomol. Chem.* **2004**, *2*, 1–16.
- [31] G. W. Kabalka, H. C. Hedgecock Jr., *J. Org. Chem.* **1975**, *40*, 1776–1779.
- [32] CCDC-782614 contains the supplementary crystallographic data for compound **86**. These data can be obtained free of charge from The Cambridge Crystallographic Data Centre via [www.ccdc.cam.ac.uk/data\\_request/cif](http://www.ccdc.cam.ac.uk/data_request/cif).

Received: September 13, 2010

Published Online: November 23, 2010